



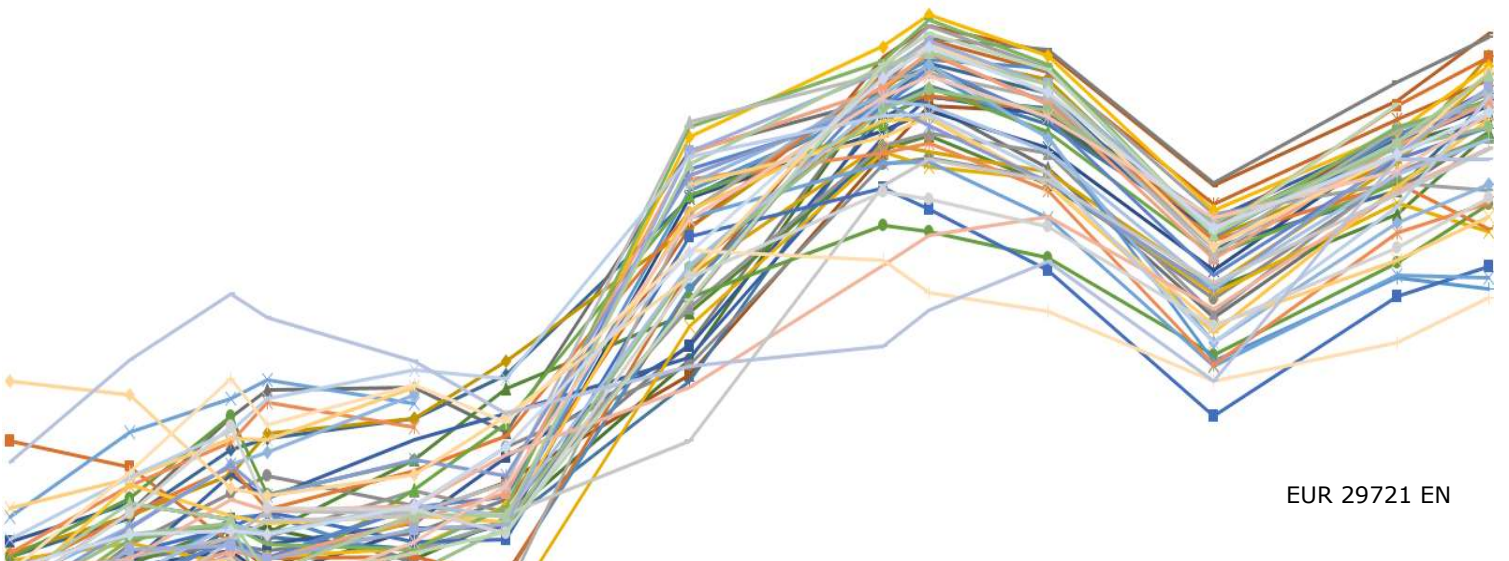
JRC TECHNICAL REPORTS

Applicability limits of Sentinel-2 data compared to higher resolution imagery for CAP checks by monitoring

CASE STUDY

Vajsova B., Fasbender D., Wirnhardt C.,
Lemajic S., Sima A., Åstrand P.

2019



This publication is a Technical report by the Joint Research Centre (JRC), the European Commission's science and knowledge service. It aims to provide evidence-based scientific support to the European policymaking process. The scientific output expressed does not imply a policy position of the European Commission. Neither the European Commission nor any person acting on behalf of the Commission is responsible for the use that might be made of this publication.

Contact information

Name: Blanka Vajsova
Address: Via E. Fermi 2749, TP 272
Email: blanka.vajsova@ext.ec.europa.eu
Tel.: +39 0332 78 6170

EU Science Hub

<https://ec.europa.eu/jrc>

JRC115564

EUR 29721 EN

PDF ISBN 978-92-76-01935-0 ISSN 1831-9424 doi:10.2760/26277

Ispira: Publications Office of the European Union, 2019

© European Union, 2019

The reuse policy of the European Commission is implemented by Commission Decision 2011/833/EU of 12 December 2011 on the reuse of Commission documents (OJ L 330, 14.12.2011, p. 39). Reuse is authorised, provided the source of the document is acknowledged and its original meaning or message is not distorted. The European Commission shall not be liable for any consequence stemming from the reuse. For any use or reproduction of photos or other material that is not owned by the EU, permission must be sought directly from the copyright holders.

All content © European Union, 2019, except: pages:12, 13, 14,22,23 Images used in figures, courtesy of Planet Labs,Inc.,2018, figure 8, figure9, figure10, figure15, figure16, figure17, figure18

How to cite this report: Vajsova B., Fasbender D., Wirnhardt C., Lemajic S., Sima A., Åstrand P., Applicability limits of Sentinel-2 data compared to higher resolution imagery for CAP checks by monitoring, EUR 29721 EN, Publications Office of the European Union, 2019, ISBN 978-92-76-01935-0, doi:10.2760/26277, JRC115564

Contents

1	Introduction	1
1.1	Background and context.....	1
1.2	Objective	1
1.3	Concept	1
2	Theoretical assumptions	1
2.1	Assumptions based on practices.....	1
3	Methodology.....	2
3.1	Data selection.....	2
3.1.1	HHR image data	2
3.1.2	Tested area	3
3.1.3	Vector data sample	4
3.2	Technical aspects	5
3.2.1	Image data	5
3.2.2	Geometric positional accuracy versus spatial overlay	10
3.3	Methodology for evaluation of results.....	13
3.3.1	An expert judgement.....	13
3.3.2	Estimation of the correlation coefficient between a pair of NDVI time series 14	
3.3.3	Model	15
4	Validation	17
5	Results	19
5.1	Selected examples	19
5.2	Evaluation analysis.....	21
5.2.1	Evaluation based on the expert judgement.....	21
5.2.2	Evaluation based on the statistical assessment	21
6	Discussion & Conclusions	28
6.1	Summary of specific findings related to the sample:	28
6.2	General conclusions and discussion	28

1 Introduction

1.1 Background and context

The Common Agricultural Policy (CAP) 'checks by monitoring' are replacing the on-the-spot-checks presently used to verify that the area-based direct aid is granted correctly to EU farmers. The method is implemented as of application year 2018 through Article 40a of the implementing regulation (EU) 809/2014. Such checks rely on automatic methods to observe and assess the CAP eligibility criteria, commitments and obligations using the Copernicus Sentinel imagery or equivalent, making use of automated data processing and advanced data analysis methods (i.e. machine learning), coupled with an efficient handling of farmer aid applications.

In the case where the spatial resolution of above mentioned imagery is not sufficient to conclude on the eligibility or holding compliance (i.e. due to small size of the parcels belonging to the dossier), the competent authority must undertake appropriate 'follow up activity', e.g. by requesting additional information from the beneficiaries, or by making use of 'time stacks' of information derived from a higher resolution image source (i.e. HHR: High High Resolution satellite imagery with a ground sampling distance approximately two or more times better than the Sentinel-2).

The very high number of the 'follow up activities' required to conclude on holding compliance that could possibly result for fragmented landscapes with numerous small parcels is among the major concerns of the EU Member States (MS) towards the operational implementation of checks by monitoring. However the extra effort related to checks of small parcels should be always put in the context of their relevance to conclude on the payment of the given farmer dossier and can be estimated based on the so-called "sifting" preparatory operation [1]. At the end of this iterative process, the set of "small" parcels that should be checked with alternative methods will be known.

Because it is linked with extra costs and efforts, understanding when the use of HHR imagery is effective (i.e. adequate to accomplish its purpose), and provides enhanced information, superior to that extracted from the coarser resolution imagery is a key factor of efficiency in checks by monitoring.

1.2 Objective

The objective of this case study is therefore to understand better and summarize what the performance potential of Sentinel-2 is with respect to the small parcels as well as to estimate the HHR data amount needed to cover the information gap caused by the course Sentinel-2 resolution.

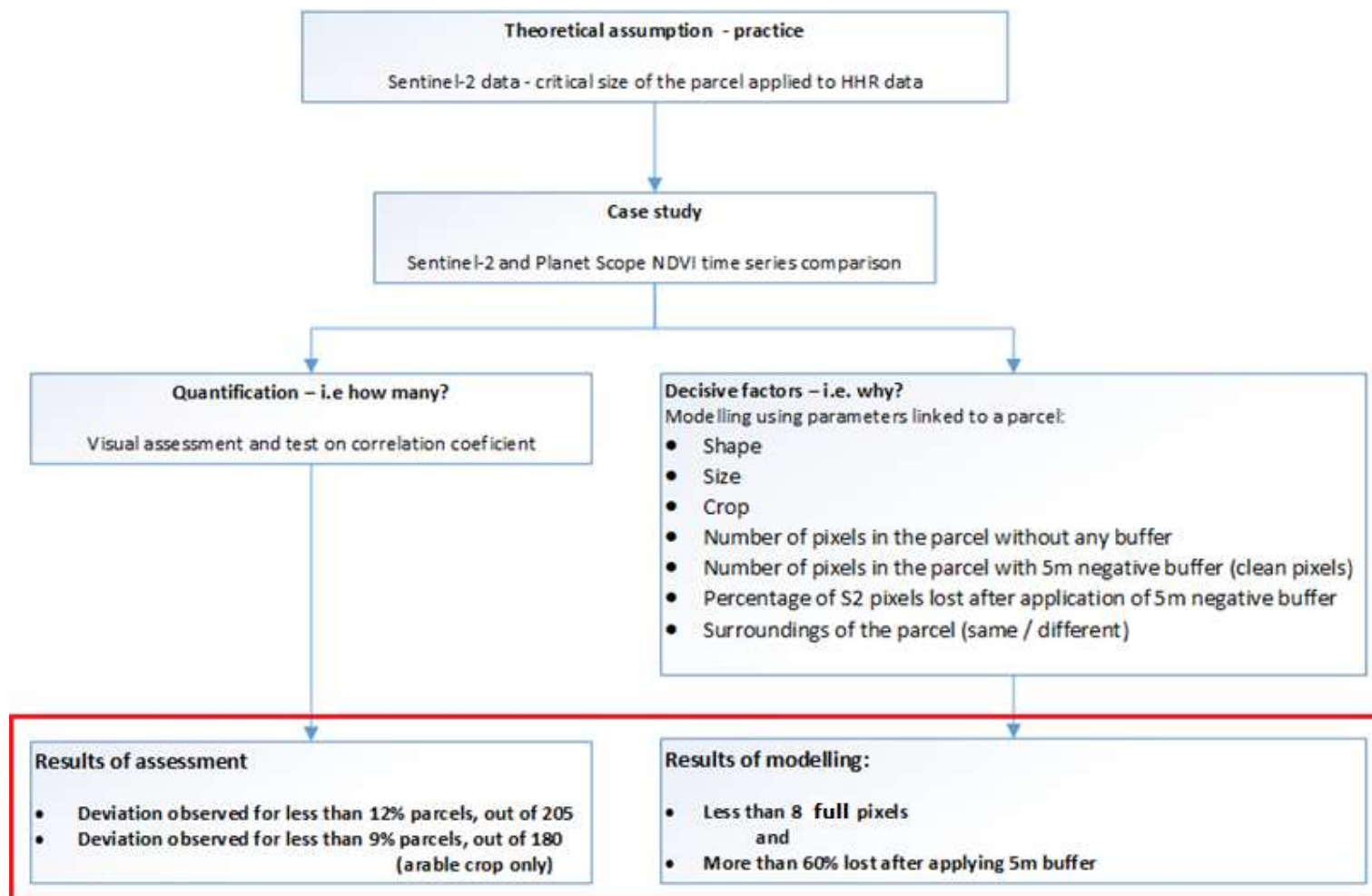
The main goals of the case study were (i) to quantify the applicability limits of Sentinel-2 and to estimate the benefit of HHR imagery (ii) to fine-tune the limits of Sentinel-2 imagery through the use of geospatial parameters of parcels, both in the frame of the CAP checks monitoring.

1.3 Concept

The concept is based on three consecutive steps. First, following the experience thresholds we extracted the sample of parcels having size below or equal to 0.5ha and created NDVI time series using Sentinel-2 and other HHR data. To understand how big portion from our sample would need another source of information to complement the Sentinel-2 data we carried out a visual and statistical assessment of couples of NDVI time series, described in chapters 3.3.1 and 3.3.2. At the end applying a statistical modelling, we evaluated the correlation between various parameters of parcels and the correlation coefficient of similarity, chapter 3.3.3. In this way, we were able to set limiting threshold parameters using those geospatial factors we thought are decisive for the sensor performance, i.e to provide information necessary to make a conclusion on the status and activity on the parcel.

The limiting parameters of parcel indicate threshold for which there is a high probability to observe discrepancies in the performance of Sentinel-2 compared to other HHR sensor, in our case PlanetScope.

Figure 1. Concept of case study



2 Theoretical assumptions

2.1 Assumptions based on practices

Ideal regular shape is taken into account:

Concerning the size of 'small' parcels, based on MSs' previous experience with Sentinel-2 (S2) imagery used during CAP checks or other pilot projects two critical thresholds were set (summarised in Table 1.).

Table 1. Setting critical thresholds on parcels size for Sentinel-2 data

SENTINEL-2	Size of the parcel [ha]	Number or pixels inside the parcel (approx.)	Note
	> 0,5	> 49	Parcel 'monitorable' by S2 independently on the shape of the parcel
1.Critical threshold	0,5	49	Depends on the shape and position (or other factors) of the parcel
2.Critical threshold	0,3	25	
	< 0,3	< 25	S2 does not give satisfactory results

Considering the ground sampling distance (GSD) and number of pixels inside the parcel (without any buffer applied), analogically, theoretical critical thresholds were calculated for HHR (3.125m GSD) imagery. These critical size thresholds are only indicative (regular shape considered) but might determine the size of the parcel where even HHR imagery could face difficulties in crop/agriculture activity identification.

Table 2. Setting critical thresholds on parcels size for HHR data

HHR (3.125m GSD)	Size of the parcel [ha]	Number or pixels inside the parcel (approx.)	Note
	> 0.048	> 49	Parcel 'monitorable' by HHR imagery independently on the shape of the parcel
1.Critical threshold	0,048	49	Result depends on the shape and position (or other factors) of the parcel
2.Critical threshold	0,024	25	
	< 0,024	< 25	HHR imagery does not give satisfactory results

3 Methodology

For the purpose of the study the mean NDVI time series of S2, calculated over the number of parcels of various geospatial characteristic, were compared with the mean NDVI time series of a selected HHR sensor.

Through the visual and the statistical assessment of a similarity between NDVI time series of these two satellite data we aimed to find out:

1. For how many parcels from the selected sample the NDVI time series do not prove the similarity, i.e S2 data fails (is significantly different than the signal of HHR)
2. By analysing the relations between the similarity of signals and different geospatial characteristics of parcels to address the decisive factor(s) influencing the capability of S2 to provide sufficient information about particular continuous state or a change of the state of the land phenomenon.

The statistical assessment of similarity was based on correlation coefficient, more information on the evaluation criteria are given in section 3.3.

The studied geospatial characteristics/parameters of the parcel were:

- Shape of the parcel (regular if the shape is close to a square, different elongations of rectangles or irregular)
- Size of the parcel
- Crop type
- Number of pixels in the parcel without any buffer
- Number of pixels in the parcel with 5m negative buffer (i.e. pure/full pixels)
- Percentage of S2 pixels lost after application of 5m negative buffer
- Surroundings of the parcel (same / different, building...)

3.1 Data selection

3.1.1 HHR image data

Since HHR satellite data should serve as a source of additional information (i.e. superior to S2 data) the requirements on ground sampling distance are stricter, i.e. GSD approximately two or more times better than S2, however the temporal resolution should be at least equivalent to the one of S2 (i.e. revisit time on weekly basis). Because in the monitoring context the signal variation will be expressed in a form of composite indicators (for instance agriculture indices), there is a need to have at least 4 spectral bands (Red, Green, Blue, Near Infra-Red) similar to the one of S2.

For the purpose of our case study we decided to use PlanetScope satellites data due to availability of the rich archive of image data covering with the dense temporal resolution the whole EU territory. That enabled us to select testing area according to our needs and possibilities (complementary information available i.e vectors, crops..).

Basic requirements:

- Temporal resolution at least on weekly basis
- GSD < 5m
- 4 spectral bands
- Data services available/planned (either through own platform or through DIAS)

Comparison of data availability between S2 and PlanetScope

Search criteria:

- Acquisition window: start date 01/02/2018 , end date 21/09/2018
- AOI 100% coverage
- Cloud cover % (0, 50, 100)

- Source (S2, PlanetScope ortho tile)
- Country: Netherlands

Table 3. Availability of the products according to the search criteria

	S2 <0%cc	S2 <50%cc	S2 all	PlanetScope 0%cc	PlanetScope 50%cc	PlanetScope all
Nr. of available acquisitions	10	40	85	50	109	171
Average temporal resolution (days)	20	5.64	2.65	4.55	2.15	1.36
Max. gap between two acquisitions (days)	55	20	10	20	12	5
Available time frame between first and last capture	180	220	223	223	230	231

For charts displaying the data availability for both sensors, see the ANNEX A.

3.1.2 Tested area

The country selected for the study is Netherlands due to an open and free access to the Land Parcel Identification System (LPIS) and related farmers' declarations.

In order to optimize the image use, two different AOIs (AOI -1, AOI - 2) were selected, for which two sets of cloud free PlanetScope ortho tiles were downloaded. The selection of concrete AOIs was based on the following parameters:

- AOI is within one S2 tile
- AOI covers representative sample of selected crop (see chapter below).

Figure 2. Position of the AOIs in Netherlands



3.1.3 Vector data sample

For the definition of geometric boundaries of agriculture parcels we used the Geospatial Aid Application (GSAA) dataset information publicly available through the Netherlands open geo-data infrastructure [18].

In order to evaluate the impact of a parcel's geometry the sample was divided into 11 size categories (see **Table 4**). The shape of the polygon was assessed taking into account a ratio of two main sides of the parcel ($l:w$). The following types of shapes were applied: regular, irregular, $l=2w$, $l=3w$, $l=4w$ up to $l=18w$ (very elongated), see **Figure 3**.

Table 4 summarizes a distribution of all parcels used for the analysis. The shape types $l=2w \rightarrow l=18w$ were grouped in to three columns.

Figure 3. Different shape types representing the sample

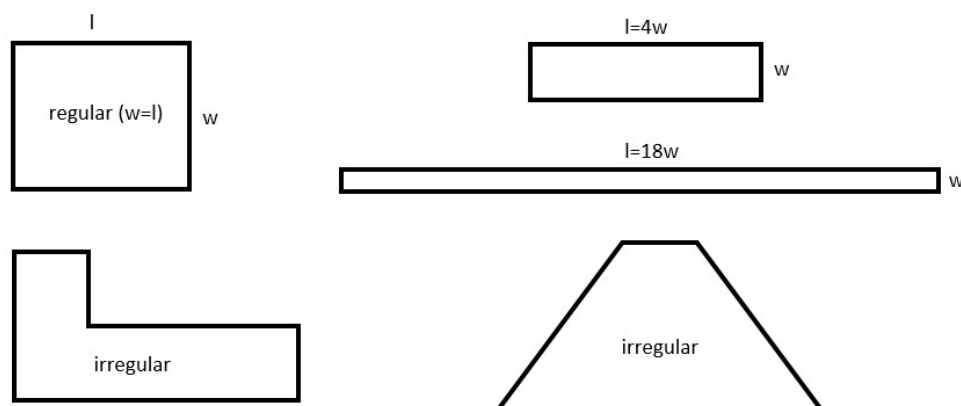


Table 4. Distribution of shape types according to the parcel size

AREA	Category	$W=l$	(2-6)	(7-	$(13-18)w=l$	Irregular	Total
0-0.01	1	0	0	0	0	0	0
0.01-	2	3	6	1	1	2	13
0.05-0.1	3	3	7	3	2	6	21
0.1-0.15	4	5	3	1	2	4	15
0.15-0.2	5	3	11	3	2	4	23
0.2-0.25	6	3	10	4	2	1	20
0.25-0.3	7	4	16	4	3	6	25
0.3-0.35	8	2	11	2	2	6	23
0.35-0.4	9	2	3	0	1	5	11
0.4-0.45	10	2	9	1	3	5	20
0.45-0.5	11	4	8	4	2	8	26
TOTAL		31	84	23	20	47	205

In total, the NDVI time series over 205 agriculture parcels for the following selected crops: maize, grass, winter wheat, sugar beet were compared (see Table 5).

Table 5. Distribution of tested crops

Crop	Number of tested parcels
Maize	29
Grass	25
Winter wheat	96
Sugar beet	55

3.2 Technical aspects

3.2.1 Image data

PlanetScope data

For the extraction of NDVI time series, the analytic ortho scene SR (surface reflectance) product was used. In order to simplify the image processing chain, only cloud free tiles (with 0% of cloud cover) were taken into consideration, which means that the full capacity of the temporal resolution was not exploited. However, taking into account a daily revisit time of PlanetScope satellites, the number of images still high enough to create NDVI time series and compare them with the S2 one.

Sentinel-2

In the study, products of both S2A and S2B satellites were used in the analysis at processing levels L2A [3] (BOA) and L1C [4] (TOA).

Table 6. Distribution of tested crops according to the processing level of Sentinel-2 data

Processing level	Crop	Number of products
L1C	Maize, Grassland	54
L2A	Winter wheat, Sugar beet	99

It is important to note that the aim of the analysis was not to compare absolute values of satellites' NDVI time series but to evaluate their similarity and capability to provide required information. Thus, both processing levels could be used for the purpose of our study.

The time span of the L1C data used in this study was set to 1/1/2018-30/8/2018 (end date depends on the current date of NDVI time series creation) in order to visualise important steps of a crop phenology. The time interval of the time series retrieved from L2A data was influenced by the availability of this product on ESA servers. The processing level L2A became an operational product only in the middle of March 2018, beginning with coverage of the Euro-Mediterranean region, with a gradual ramp-up to systematic worldwide coverage planned for the summer of 2018. For the tested AOIs, the earliest acquisition date of the L2A product available was beginning of April 2018. As from the phenology point of view March is for certain crops an important month, some of NDVI time series are affected. This however did not influence the qualitative analysis performed using these data.

While the search of the PlanetScope data was done based on 0% of cloud cover (CC) of the whole tile, the metadata search for Sentinel-2 data was set to 0% of CC over the analysed polygon (i.e search on 'clean pixels').

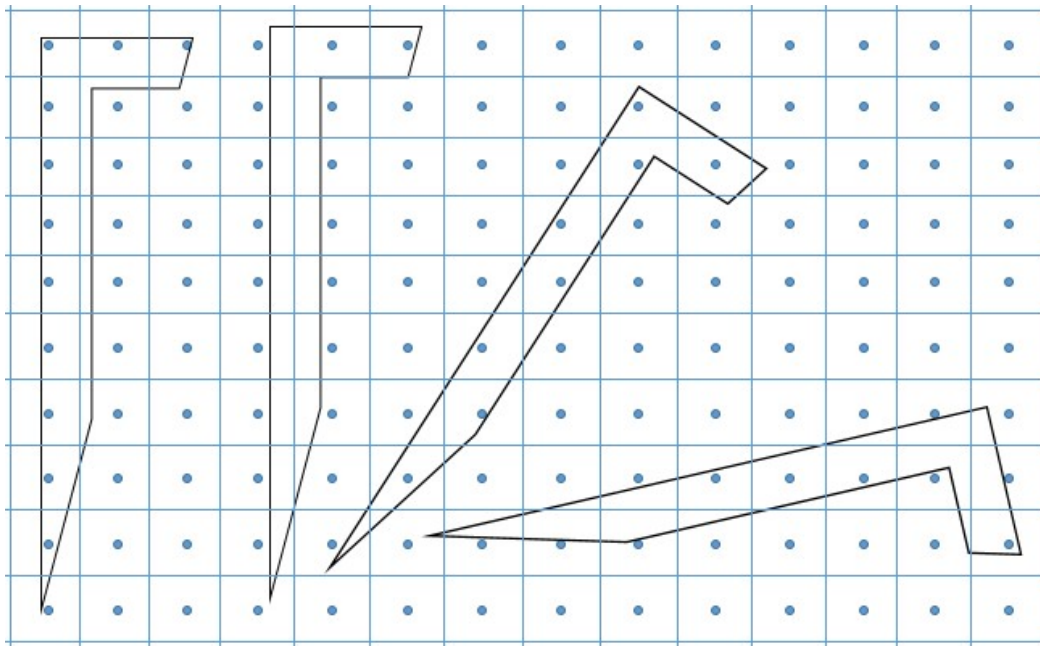
Different metadata are used for the CC assessment, depending on the processing level of the product. All Sentinel-2 products have associated cloud cover masks to simplify the user's work and to provide useful products ready to deliver. L1C cloud mask identifies cloudy pixels and separate them from those that are cloud-free. They include both dense clouds and cirrus clouds, by specifying the cloud type with an indicator. Moreover, statistical information about the percentage of dense cloud and cirrus pixels is enclosed. The overall accuracy of this CC mask is of 86.5% with tendency to underestimate the cloud cover percentage [10]. The Level-2A image data is composed of (except for others) the scene classification map (SCL) which substitutes a simple CC mask and was fully exploited in the metadata search. The SCL consists of 11 different classes at 20m and 60m resolution. Furthermore, there are associated statistics on percentage of pixels belonging to each class and quality indicators for snow and cloud probability. The SLC is of higher quality than the simple CC mask added to L1C data and therefore only a little human intervention was necessary to get cloud free stacks of S2 time series compared to working with L1C in combination with its CC mask. The average overall accuracy for 14 classification products reached $81.1 \pm 14.1\%$. The recognition of clear pixels over land and water reached overall accuracy of 91.5% [11]

3.2.1.1 Number of pixels covering a parcel, and a buffer

The number of pixels that are inside the parcel is an important factor that could have an impact on the assessment. Many methods exist to calculate this number. The concept used in this study is based on a sum of all raster cells whose centres are within the polygon. A disadvantage of this method is that the number of pixels is not only a function of the size and the shape of the parcel, but it is very sensitive to a relative position of the raster regards to an overlaid vector layer (see

Figure 4).

Figure 4. Position of the parcel on the raster and different number of pixels inside the parcel

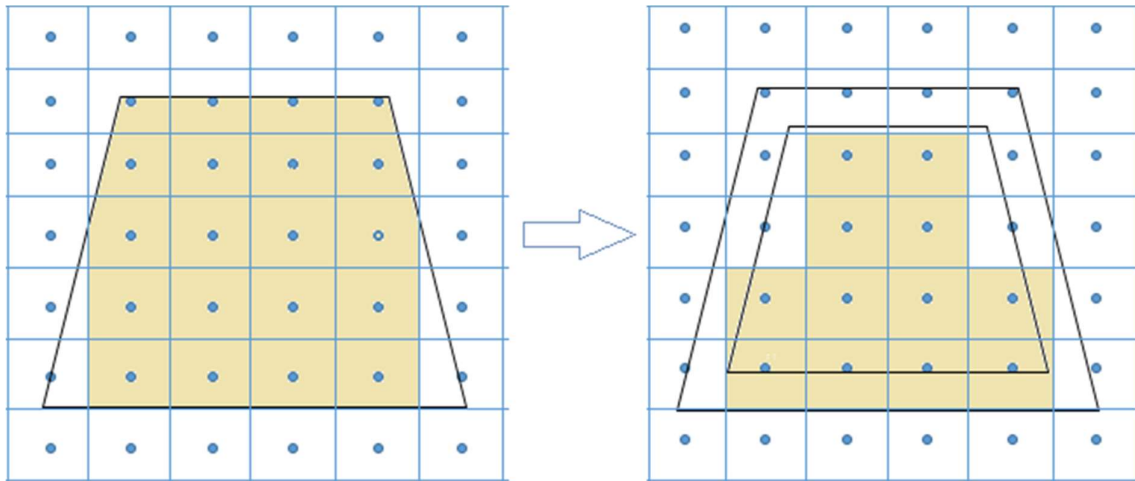


In order to eliminate the influence of neighbouring parcels and mixed pixels i.e. pixels on the border of parcels that contain also a spectral information belonging to areas outside

the parcels, a buffer of $(0.5 \times \text{pixel size})\text{m}$ was introduced at the beginning of the study to treat this issue. As the study deals with the small parcels, some of them were considered without any buffer (0m buffer) in order to keep at least one pixel inside the boundary, see an example **Figure 5**.

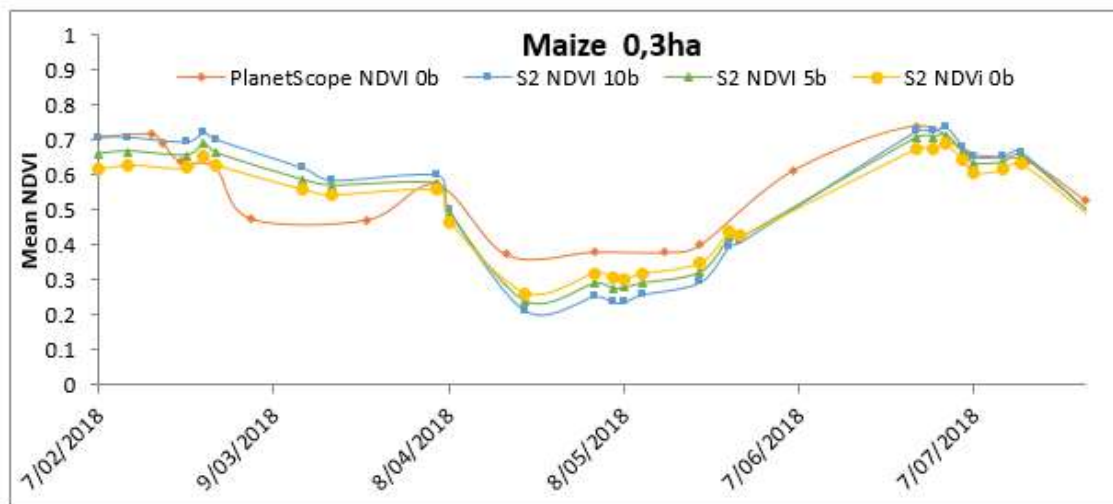
With the introduction of the buffer a new factor was implemented which is defined as a number of 'full' pixels inside the agriculture parcel.

Figure 5. Example of the negative buffer and the subsequent number of full pixels



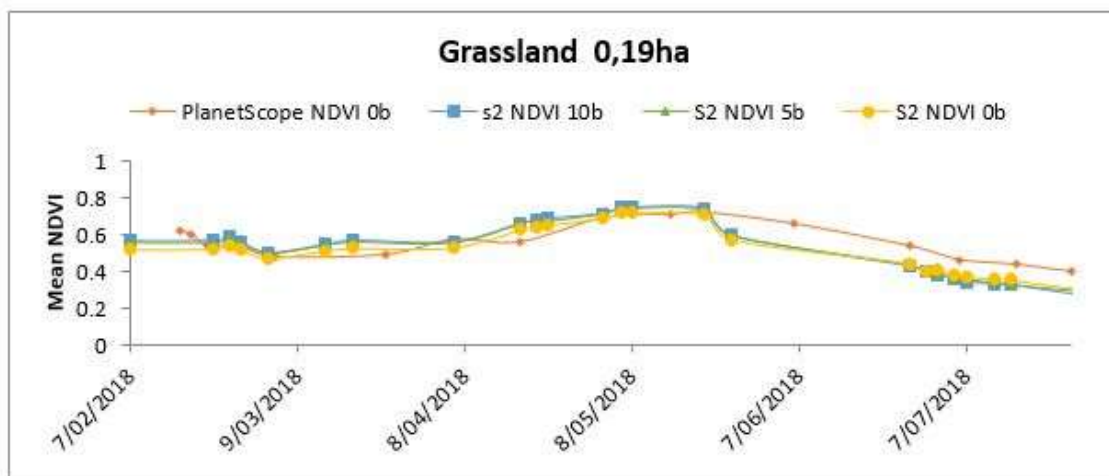
Furthermore, an investigation regarding an influence of a buffer size on NDVI time series was performed (see some examples in **Figure 6** and **Figure 7**).

Figure 6. Influence of negative buffer on the mean NDVI time series – Maize



Sensor	Buffer [m]	N. pixels
Planet Scope	0	327
S2	0	29
S2	5	20
S2	10	11

Figure 7. Influence of the negative buffer on the mean NDVI time series - Grassland



Sensor	Buffer [m]	N. pixels
Planet Scope	0	205
S2	0	18
S2	5	10
S2	10	5

Results of experimenting with various buffer settings show that although slightly different absolute mean NDVI values are observed the curvatures of NDVI time series keep the same behaviour. The fact that the curvature do not substantially change the shape while using various buffers is important in the context of the study, because the correlation coefficients of the NDVI time series are compared.

3.2.1.2 NDVI index calculation

NDVI index was calculated applying the standard formula:

$$NDVI = \frac{NIR - RED}{NIR + RED}$$

The following bands were used:

PlanetScope: band 4 (NIR) and band 3 (RED)

central wavelengths: 860nm NIR and 670nm RED band [15]

Sentinel-2: band 8 (NIR) and band 4 (RED)

central wavelengths: 842nm NIR and 665nm RED band [2]

3.2.1.3 Software

PlanetScope data were downloaded through the Planet Explorer platform using metadata filters. The downloaded Analytic Ortho Scene [5] products were mosaicked for each acquisition date. The example shown below is a mosaic of 7 ortho scene images.

Figure 8. False colour composite (RGB 421) of a PlanetScope image acquired on 15/05/2018 over AOI-1 mosaicked from 7 ortho scene tiles.

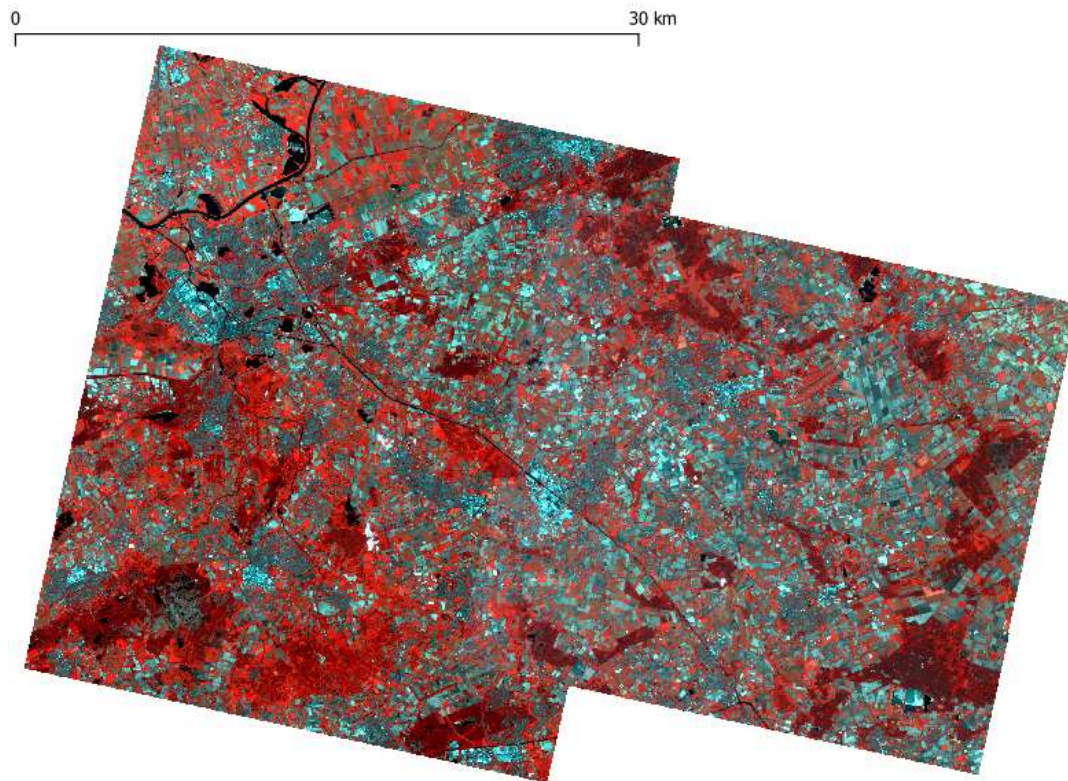
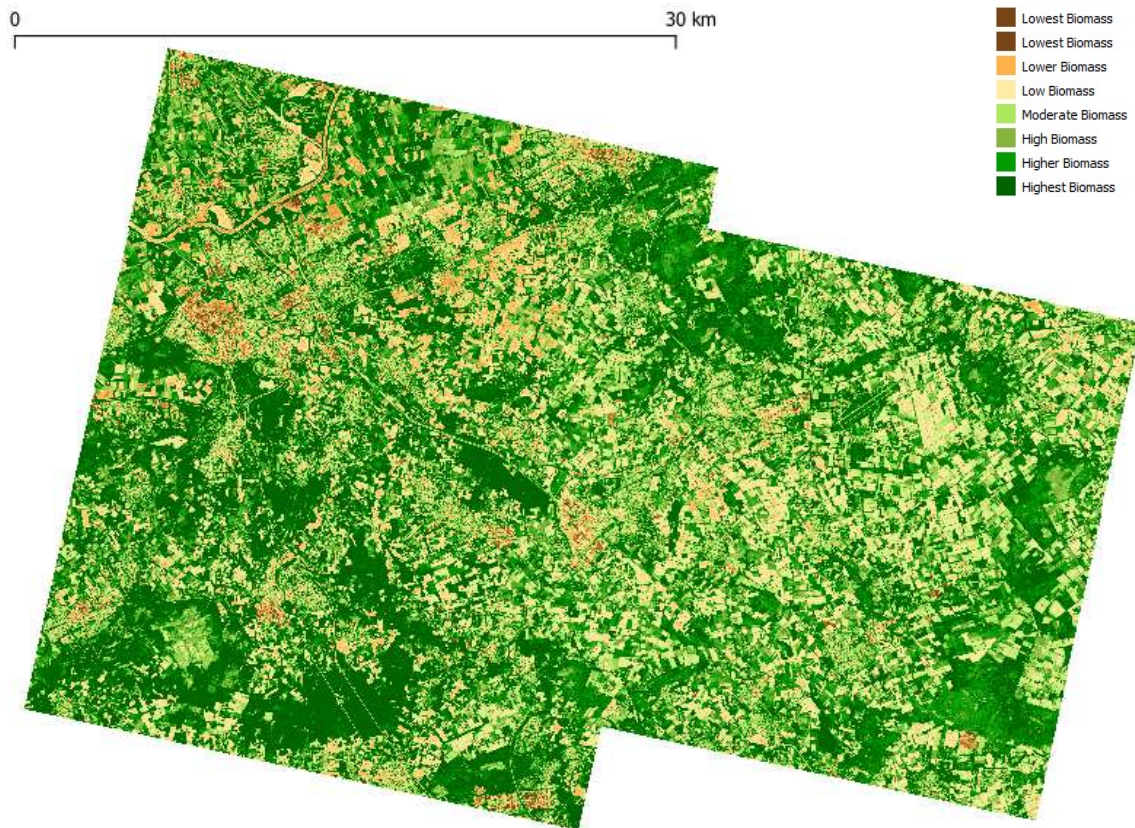


Figure 9. NDVI image calculated from Planetscope data acquired on 15/05/2018 over AOI1



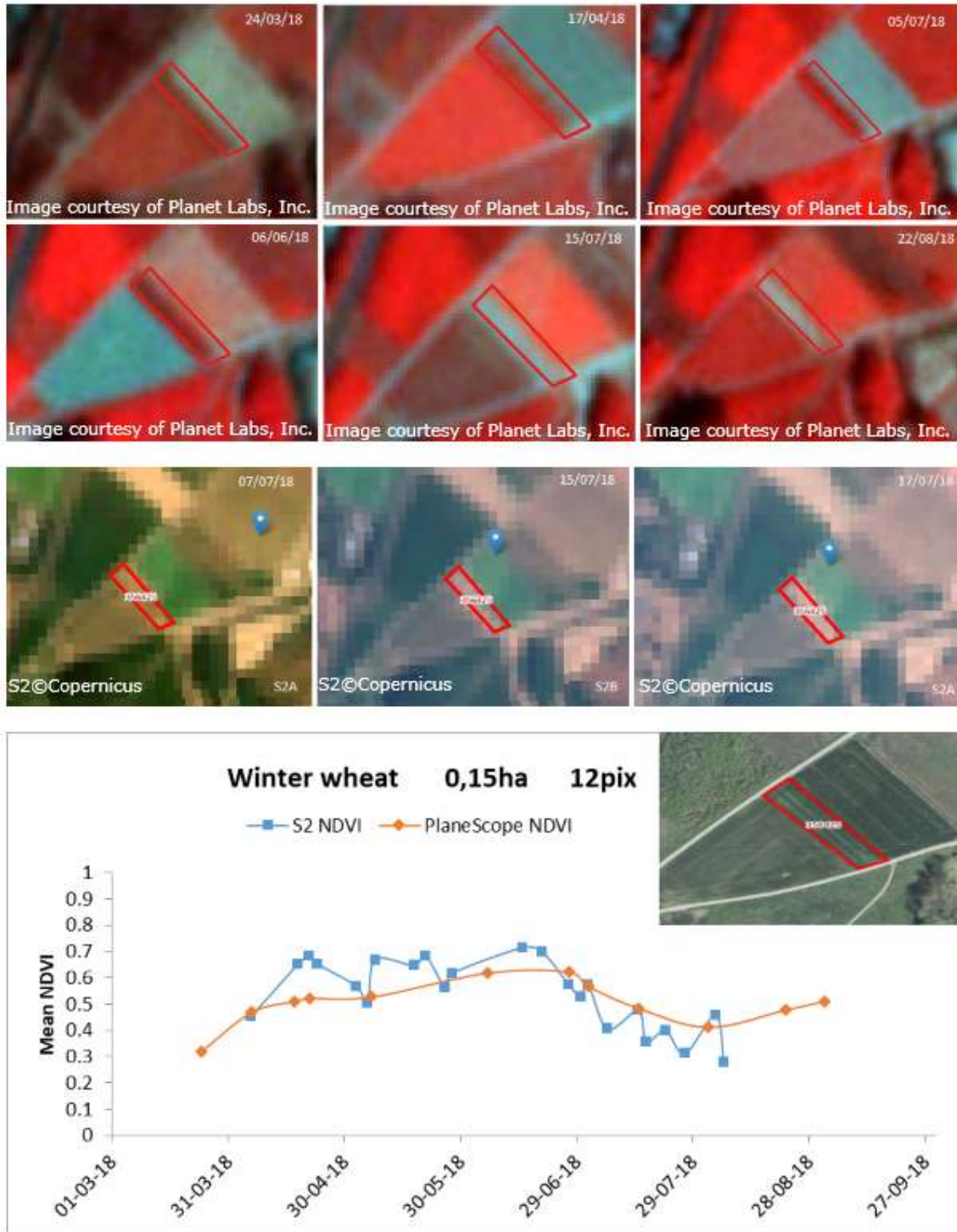
The calculation of Planetscope NDVI images and the extraction of mean NDVI time series were performed by in-house developed python scripts using the built-in raster calculator [6] and zonal statistics [7] functionalities of the open source QGIS [8] software.

S2 NDVI time series extraction was performed in the Joint Research Centre Earth Observation Data and Processing Platform (JEODPP). JEODPP is a versatile petabyte scale platform providing a cluster environment for batch processing, a web-based remote desktop access with a variety of software suites, and a web-based interactive visualisation and analysis ecosystem. For more information see [12].

3.2.2 Geometric positional accuracy versus spatial overlay

Information derived from two different spatial data sets are comparable and can be used together for spatial analysis if their specification is well-known and if their quality (spatial accuracy/precision, temporal accuracy) is well recorded. Quality issues present in the source layers will certainly affect any results from their integration [13]. This fact has to be considered, especially in the context of small parcel analysis, because the smaller the parcel is the bigger the impact of the positional inaccuracy is on the correctness of NDVI time series retrieved from that parcel.

Figure 10. Example of the geometric positional inaccuracy of raster data



From **Figure 10** it is evident that PlanetScope imagery is shifted 5-7m South-West with respect to the parcel outline (correctly positioned in the VHR image). Consequently, 30% of polygon from which the time series were retrieved covers pixels of the neighbouring parcels sown with different crops. A similar situation can be observed for the S2 imagery. Out of the 3 images in **Figure 10**, 2 are georeferenced correctly however the image captured by S2B is effected by a shift. All these discrepancies negatively influence and bias the NDVI time series.

3.2.2.1 Vector data

The minimum accuracy requirement for the LPIS being a reference frame for the GSAA, is defined in Article 70. of Regulation (EU) 1306/2013 as at least equivalent to that of cartography at a scale of 1:10.000 and, as from 2016, at a scale of 1:5.000. This translates into [13]:

- a horizontal absolute positional accuracy expressed as RMSE of 1.25m (5.000 x 0.25mm = 1.25m), or the equivalent value CE(95)of 3.06m.
- display range and feature type content compatible with a map with a scale 1:5.000 (i.e. topographic maps rather than urban survey maps),
- using orthoimagery ≤ 0.5 m GSD.

3.2.2.2 PlanetScope image data

Requirements

According to the PlanetScope Analytic Ortho Scene Product Specifications the requirements on the geometric quality is designed for a wide variety of applications that require imagery with an accurate geolocation and cartographic projection. The positional accuracy declared is less than 10 m RMSE_{2D} [14].

The product has been processed to remove distortions caused by terrain and can be used for many data science and analytic applications. It eliminates the perspective effect on the ground (not on buildings), restoring the geometry of a vertical shot. The imagery has radiometric corrections applied to correct for any sensor artefacts and transformation to at-sensor radiance. In addition, the imagery has atmospheric corrections applied to account for atmospheric, surface and spectral conditions and geometry when converting top of atmosphere reflectance to surface reflectance [14].

Actual performance

The absolute positional accuracy test has been performed by JRC [15] on the Planet Analytic Ortho Tile products comparing image coordinates and coordinates of ground control points (GCPs) measured directly in the field with the GNSS device. The RMSE_{1D} of GCPs is below 0.5m

The geolocation performance of the PlanetScope's Level 3A:

- max RMSE_x=5.18m and max RMSE_y=4.21m
- max CE(90)=9.93m

3.2.2.3 Sentinel-2 image data

Requirements

According to the Sentinel-2 Calibration and Validation Plan for the Operational Phase, the geometric quality requirement for absolute geolocation uncertainty of Level-1C product with respect to a reference map shall be better than 12.5 m at 2σ confidence level with the need of GCPs.

Regarding the accuracy of the multi-temporal registration of the Level 1-C products, the ESA's objective is to achieve co-registration accuracy better than 3 meters (0.3 pixels) at 95.5% confidence level. This will be applicable only after activation of the geometrical refinement. The refinement step will be activated upon completion of the Global Reference Image (GRI) and the final validation of the refining algorithm. The elaboration of the GRI and the DEM benchmarking is currently on-going. The finalisation of the reference geometry and the activation of the orbit refinements are now foreseen for Q3 2019

The band coregistration requirement was set to <0.3 pixel at 99.7% confidence level.

Actual performance

According to the Data Quality Report from 08/10/2018 (end of testing period)[11],

- Absolute geolocation accuracy (without ground control points) resulted closer to 11m at 95% confidence level. However, geolocation accuracy for S2B was not stable in the time of the test. A new geometric calibration has been implemented on 18/09/2018, after this update the S2B geometric performance has shown an improvement.
- Multi-temporal performance taken as the 95% percentile of the mean error value for all tiles measured on the reference band (B04) was 11 m for S2A and 13 m for S2B. The co-registration error was within one pixel for 92% of S2A and 86% of S2B products. Still for 6% of S2A and 14% of S2B products the co-registration error was more than one pixel .
- Multi-spectral Registration less than 0.2 pixel.

3.3 Methodology for evaluation of results

In the study, we were comparing couples of NDVI time series. Each couple was composed of NDVI time series retrieved from Sentinel-2 and NDVI time series extracted from PlanetScope. Within each couple, we were assessing the similarity of these two NDVI time series. It is important to note that if we say that the couple (i.e two NDVI time series created over the same parcel) is not similar we mean by that the NDVI time series deviate.

Three main steps were performed to evaluate the results:

- 1) The similarity between the two signals was assessed for each parcel based on a visual expert judgement.
- 2) For each correlation coefficient of the two NDVI profiles, the corresponding interval of confidence was also calculated. By applying the statistical method for testing whether the correlation coefficient is larger than 0.5 with 95% of probability, we determined the parcels for which Sentinel-2 NDVI time series deviate from the ones derived from Planet Scope. This methodology is completely independent on the geospatial parameters of parcels and facilitates the understanding of the overall performance of Sentinel-2 in comparison with Planet Scope.
- 3) A model quantifying the probability of exceeding the correlation coefficient value of 0.75 was developed as a function of the number of full pixels in the parcel and the percentage of pixels that are lost after application of the 5m buffer. Based on that model, we set a limiting probability threshold as 80% for the NDVI time series deviation. Using this methodology the limiting geospatial factors of isolated parcels were defined (see below).

All three methodologies, although independent on each other and using different approach, have the same goal, i.e. to define the deviation of the NDVI time series retrieved over the same sample of data from two different image sources. All three methods gave comparable/similar conclusions.

3.3.1 An expert judgement

The NDVI time series were independently assessed by two operator, experts in the field of remote sensing, in order to determine the status of similarity (binary assessment: false/true) over each tested parcel.

3.3.2 Estimation of the correlation coefficient between a pair of NDVI time series

In this study, the correlation coefficient was chosen for assessing the similarity between the two NDVI time series derived from PlanetScope and S2. The correlation coefficients between two quantities are generally estimated using paired observations (i.e. each observation is a pair of both quantities). With paired observations, one can simply rely on the following estimator:

$$\hat{\rho} = \frac{\sum_{i=1}^n (x_i - \bar{x})(y_i - \bar{y})}{\sqrt{\sum_{i=1}^n (x_i - \bar{x})^2} \sqrt{\sum_{i=1}^n (y_i - \bar{y})^2}}$$

Where \bar{x} and \bar{y} are the observed averages of the time series and n is the number of observed pairs.

The precision of this estimator is generally evaluated using the Fischer's transformation [17].

$$\hat{\lambda} = 0.5 \ln \left(\frac{1 + \hat{\rho}}{1 - \hat{\rho}} \right)$$

The main advantage of this transformation is that $\hat{\lambda}$ is approximately following a Normal distribution with a mean equal to $\lambda = 0.5 \ln \left(\frac{1 + \rho}{1 - \rho} \right)$ (where ρ the true unknown correlation coefficient) and a variance equal to $(n - 3)^{-1}$.

One can thus build the 95% confidence interval for λ with $\hat{\lambda} \pm \frac{1.96}{\sqrt{n-3}}$ and use the inverse transformation in order to get the 95% confidence interval for

$$CI_{\rho} = \left[\frac{e^{2\hat{\lambda}_L} - 1}{e^{2\hat{\lambda}_L} + 1}; \frac{e^{2\hat{\lambda}_U} - 1}{e^{2\hat{\lambda}_U} + 1} \right]$$

Where $\hat{\lambda}_L = \hat{\lambda} - \frac{1.96}{\sqrt{n-3}}$ and $\hat{\lambda}_U = \hat{\lambda} + \frac{1.96}{\sqrt{n-3}}$.

When comparing two time series, one would also need to have both time series at the same dates. Unfortunately, this is rarely the case when the two time series are observed from two different sensors. In order to circumvent this data issue, we propose to fill the gaps by interpolating (a linear interpolation was used here) each of the time series at the observed dates of the other time series (i.e. the union of the observed dates). This approach is somewhat translating the intuitive visual comparison of the time series, while having the advantage of a sample of paired observations in order to estimate the correlation coefficient. However, this is not a genuine sample as some of the values were computed with the interpolation. So the general formula for the estimation of the variance of the estimation is not valid (i.e. we cannot take the union of the dates as the n in the variance formula). However, by using simulations, we found out that taking the number of dates in the shortest time series is a good empirical rule-of-thumb for substituting the value of n .

The choice to rely on the correlation coefficient was driven by the following expected characteristics for an index of agreement:

- It must be able to detect that the two time series share the same trend pattern;
- It should be invariant to scale and shift transformations on both time series (i.e. the actual values of time series is not important as long as the trend pattern is the same);

- It should be computed even with relatively few pairs of points (even if it will not be precise, a correlation coefficient can be computed with minimum 4 pairs of points).

While the correlation coefficient satisfies all those expectations, it is worth mentioning that it is also expected to underperform in some circumstances. Indeed, the correlation coefficient uses the averages as a pivot in order to measure the linearity between the two time series. It thus assumes that the time series have trends markedly oscillating with time around their respective averages. However, for parcels where little or no trend is expected (e.g. permanent grazed grassland and non-permanent crops), the time series should exhibit an almost constant value with few fluctuations that can be equivalent to noise.

3.3.3 Model

We built a model between the estimated correlation coefficient and the different characteristics of the sampled parcels (see Section 3). The objective of this activity is not necessarily to accurately predict if a parcel can be monitored by S2 data. It is more to better understand which are the conditions for which the S2 and PlanetScope NDVI time series do not agree, rather than simply setting a threshold on the parcel area.

We first tested some classification regression trees on agreement between the two time series (i.e. the visual or the correlation test). This method is based on an iterative definition of dichotomous split (i.e. the nodes) on the input factors so that the separation between the parcels with or without agreement is maximized. Theoretically, it has the advantage to select automatically the most relevant factors for the classification.

The factors that were present in the tree were:

- the percentage of S2 pixels lost after application of 5m negative buffer;
- the presence of the same crop in the surrounding of the parcel;
- the number of pixels in the parcel with 5m negative buffer (i.e. full pixels).

Other factors (e.g. the area or the number of pixels in the parcel without any buffer) were also included in the classification tree but they were leading to inconsistencies because the classification tries to fit a particular observation (i.e. data over-fitting). It was thus decided to discard them for the further analyses.

As a second step, we decided to model directly the estimated correlation coefficient from the three selected factors (see above). For this, we built the following linear regression model:

$$Y_i = \alpha_0 + \alpha_1 \text{SameCrop}_i + \alpha_2 \text{PurePixels}_i + \alpha_3 \text{PercLost}_i + \varepsilon_i$$

where the α_j are the parameters of the model and where for each i -th parcel:

- SameCrop_i is equal to 1 if the same crop is found in the surrounding and equal to 0 otherwise;
- PurePixels_i is the number of full pixels;
- PercLost_i is the percentage of S2 pixels lost after the 5m negative buffer;
- ε_i is an error term;
- Y_i is the transformed correlation coefficient (i.e. using the Fisher's transformation; see Section 3.3.2).

The use of the Fisher's transformation is important in order to (i) meet the normality hypothesis of the linear regression model and (ii) avoid getting non-sense correlation coefficient modelled to be larger than 1 or smaller than -1.

Using this model, we can:

- Anticipate the expected correlation coefficient for any parcel;
- Evaluate the uncertainty of this expected value;

- Evaluate the probability that the parcel's correlation coefficient will exceed a given threshold.

For any of these three applications, one must use the fitted model and rely on the inverse of the Fisher's transformation (as shown previously).

The model's parameters were estimated using ordinary least squares. The estimated values and some statistics can be found in **Table 7**.

Table 7. Estimated parameters of the regression model and their significant tests

Term	Estimate	Standard Error	t Ratio	Prob> t
(Intercept)	1.828	0.239	7.655	0.000
SameCrop	0.531	0.077	6.918	0.000
PurePixels	0.015	0.006	2.388	0.009
PercLost	-0.798	0.281	-2.834	0.003

The intercept of the model (i.e. α_0) is positive, which indicates that the correlation coefficients tend to be high for the whole dataset. The parameters for the SameCrop and for the PurePixels are significantly positive which means that having the same crop around the parcel and having more pure pixels both increase the chances to have a large correlation coefficient. On the other hand, the parameter for the percentage of pixels lost after the negative buffer is negative which indicates that the larger is the loss the smaller is the correlation coefficient.

The worst case is thus met for a parcel that (i) is not surrounded by the same crop, (ii) has no pure pixels and (iii) 100% of lost pixels after buffer application. In these conditions, the estimated correlation coefficient is equal to 0.77 and the 95% confidence interval is [0.68 ; 0.84] (the interval is not symmetric around the estimated correlation coefficient because of the inverse of the Fisher's transformation).

4 Validation

Before starting the study on the small parcels (i.e. <0.5ha) a validation test was performed for each crop over a parcel size range of 5-20ha. The assumption of the strong positive correlation between NDVI time series of S2 and PlanetScope was confirmed for each crop (See figures below).

Figure 11. Validation graph –maize

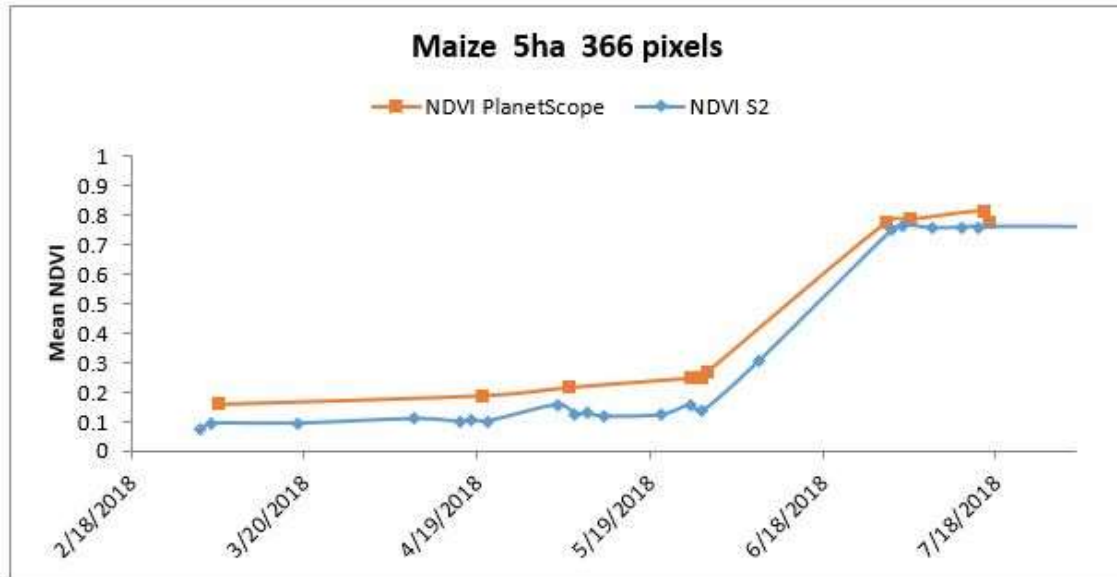


Figure 12. Validation graph -grassland

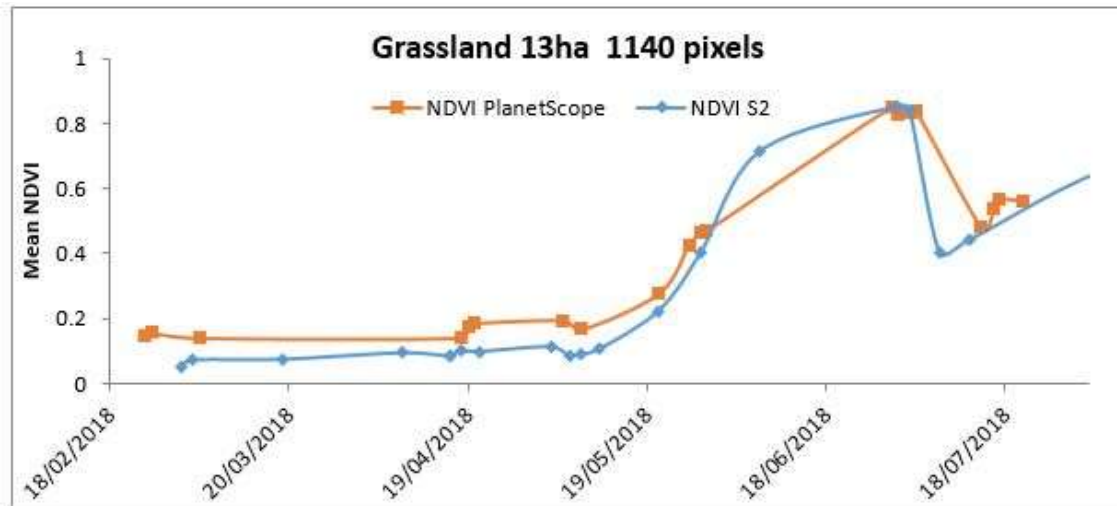


Figure 13. Validation graph – winter wheat

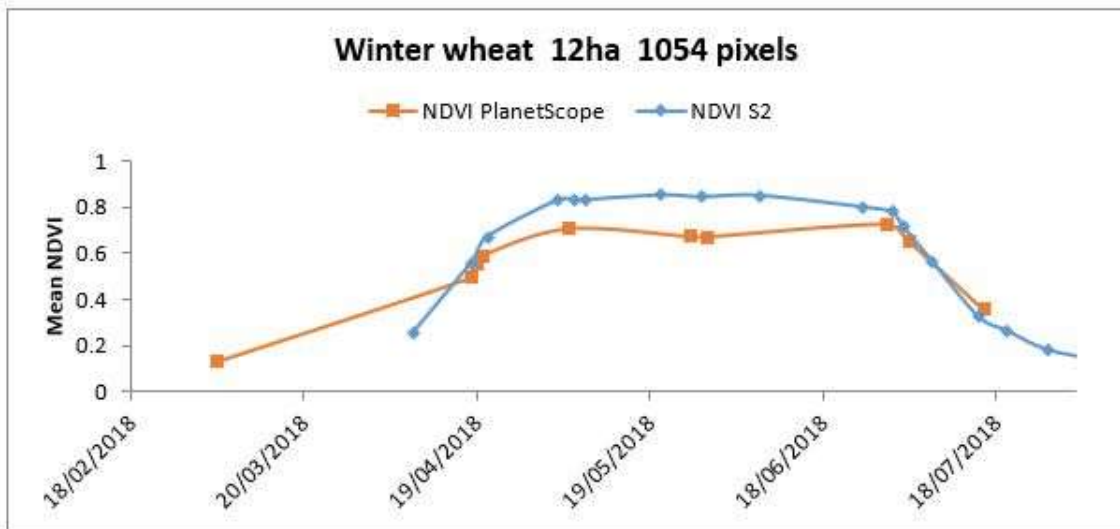
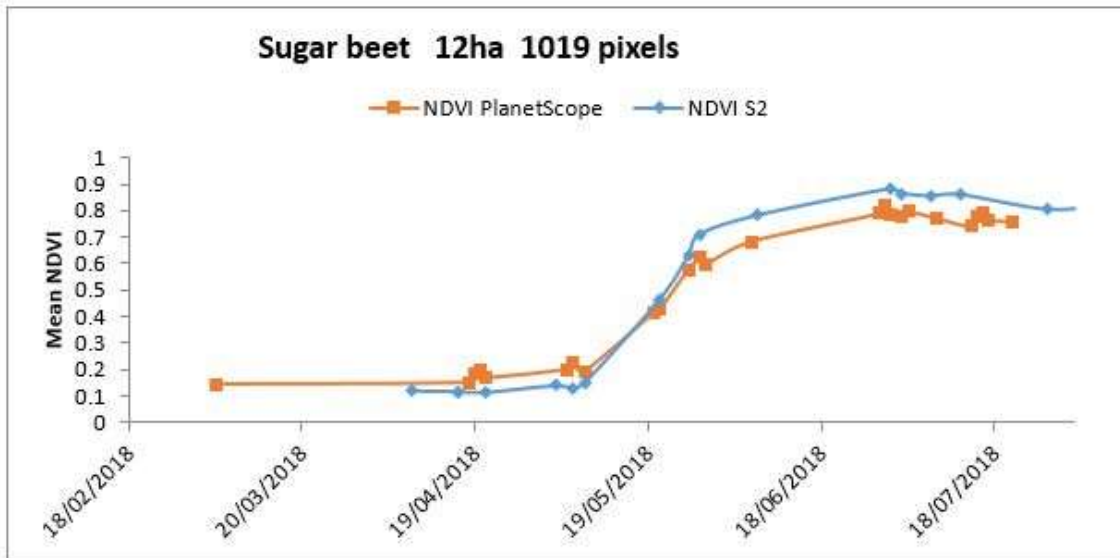


Figure 14. Validation graph –sugar beet

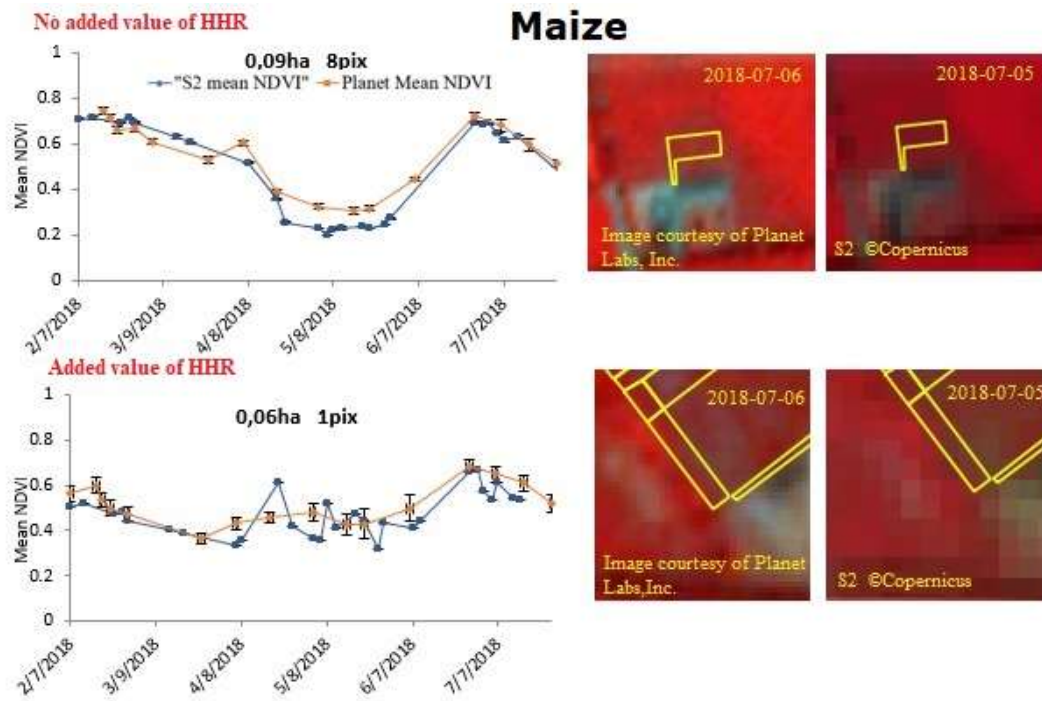


5 Results

5.1 Selected examples

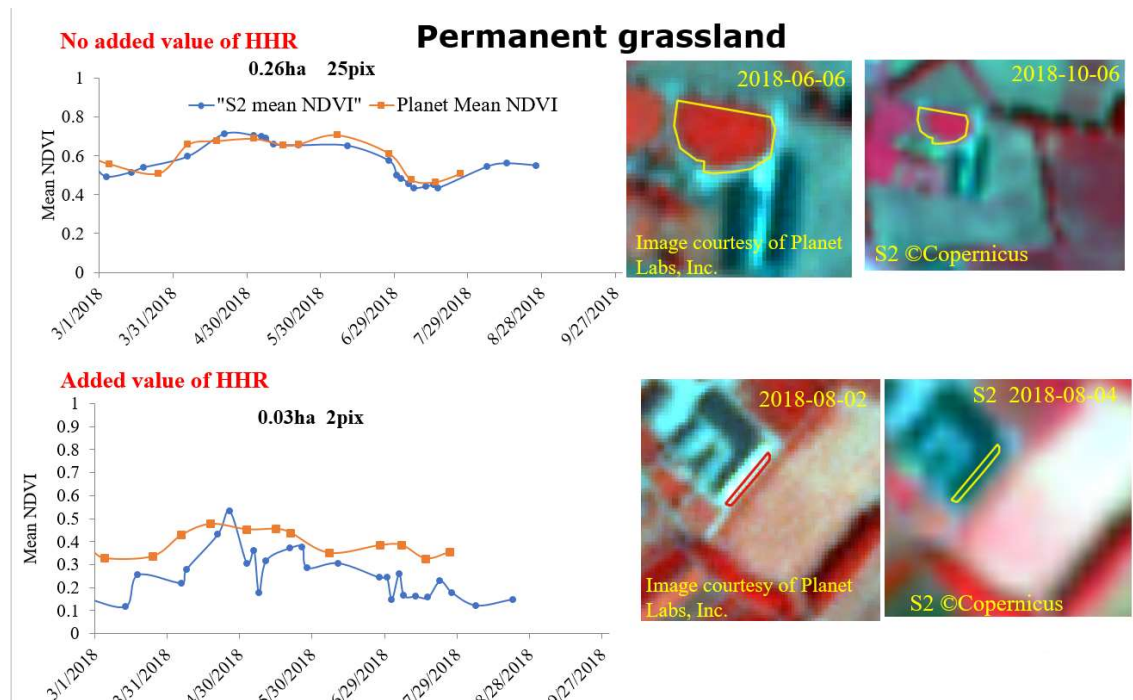
5.1.1.1 Maize

Figure 15. Example of NDVI time series – added/no added value of HHR (Maize)



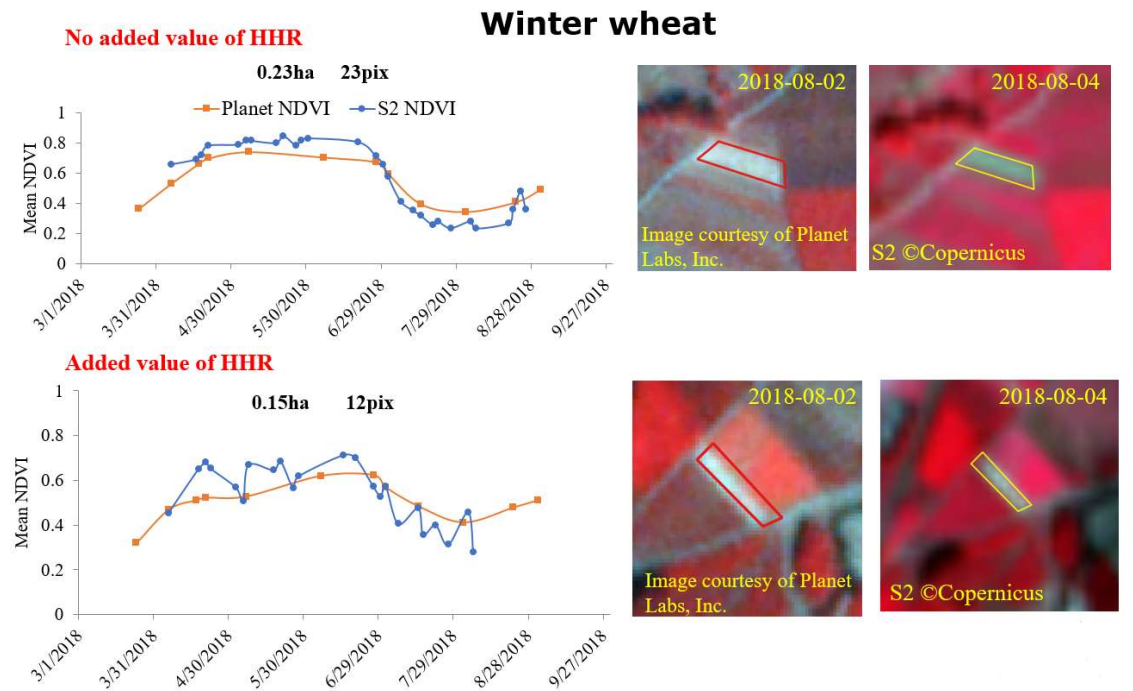
5.1.1.2 Grassland

Figure 16. Example of NDVI time series – added/no added value of HHR (Grassland)



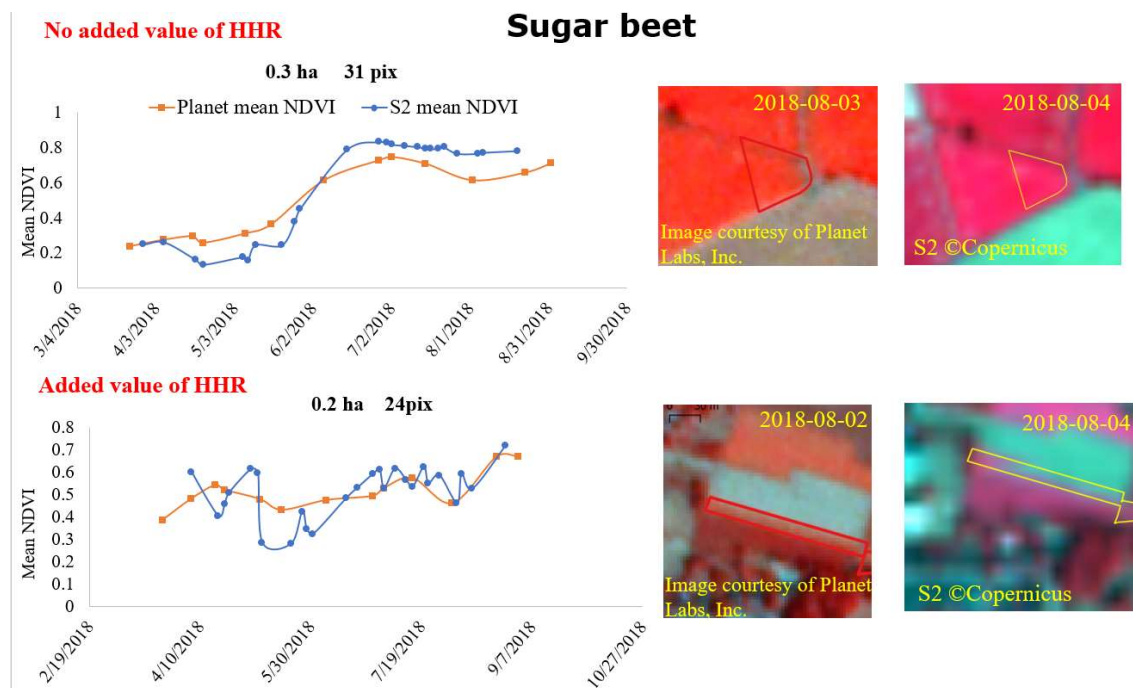
5.1.1.3 Winter wheat

Figure 17. Example of NDVI time series – added/no added value of HHR (Winter wheat)



5.1.1.4 Sugar beet

Figure 18. Example of NDVI time series – added/no added value of HHR (Sugar beet)



5.2 Evaluation analysis

Based on the visual expert judgement and statistical analysis (i.e. a method testing that the estimated correlation coefficient is larger than 0.5 with a probability of 95%) the Sentinel-2 signal deviates from the signal retrieved from Planet Scope imagery for 9% and 12% respectively, out of 205 small agricultural parcels. All HHR NDVI time series that deviate from the ones derived from S2 data bring an added value to the evaluation of markers. As no standard (typical) time series were developed for each crop/region, the benefit is assessed applying an expert judgement.

5.2.1 Evaluation based on the expert judgement

Table 8. The summary assessment table based on the visual assessment - number of parcels where the signal of Sentinel-2 deviates from the Planet's signal

Crop	Same results with Sentinel-2 and Planet	Sentinel-2 deviates from Planet's signal	% Sentinel-2 deviates from Planet's signal
Grassland	22	3	12%
Maize	27	2	7%
Sugar beet	51	4	7%
Winter wheat	86	10	10%
Total	186	19	9%

5.2.2 Evaluation based on the statistical assessment

Table 9. The summary assessment table based on the statistical assessment - % of parcels where the signal of Sentinel-2 deviates from the Planet's signal

Crop	Same results with Sentinel-2 and Planet	Sentinel-2 deviates from Planet's signal	% Sentinel-2 deviates from Planet's signal
Grassland	16	9	36%
Maize	24	5	17%
Sugar beet	50	5	9%
Winter wheat	91	5	5%
Total	181	24	12%

Figure 19. Graph of the correlation coefficient (colour scale) as a function of the shape of the parcels and the % of S2 pixels lost after application of 5m negative buffer. Top: isolated parcels surrounded by different crops; bottom: parcels with the same crop around

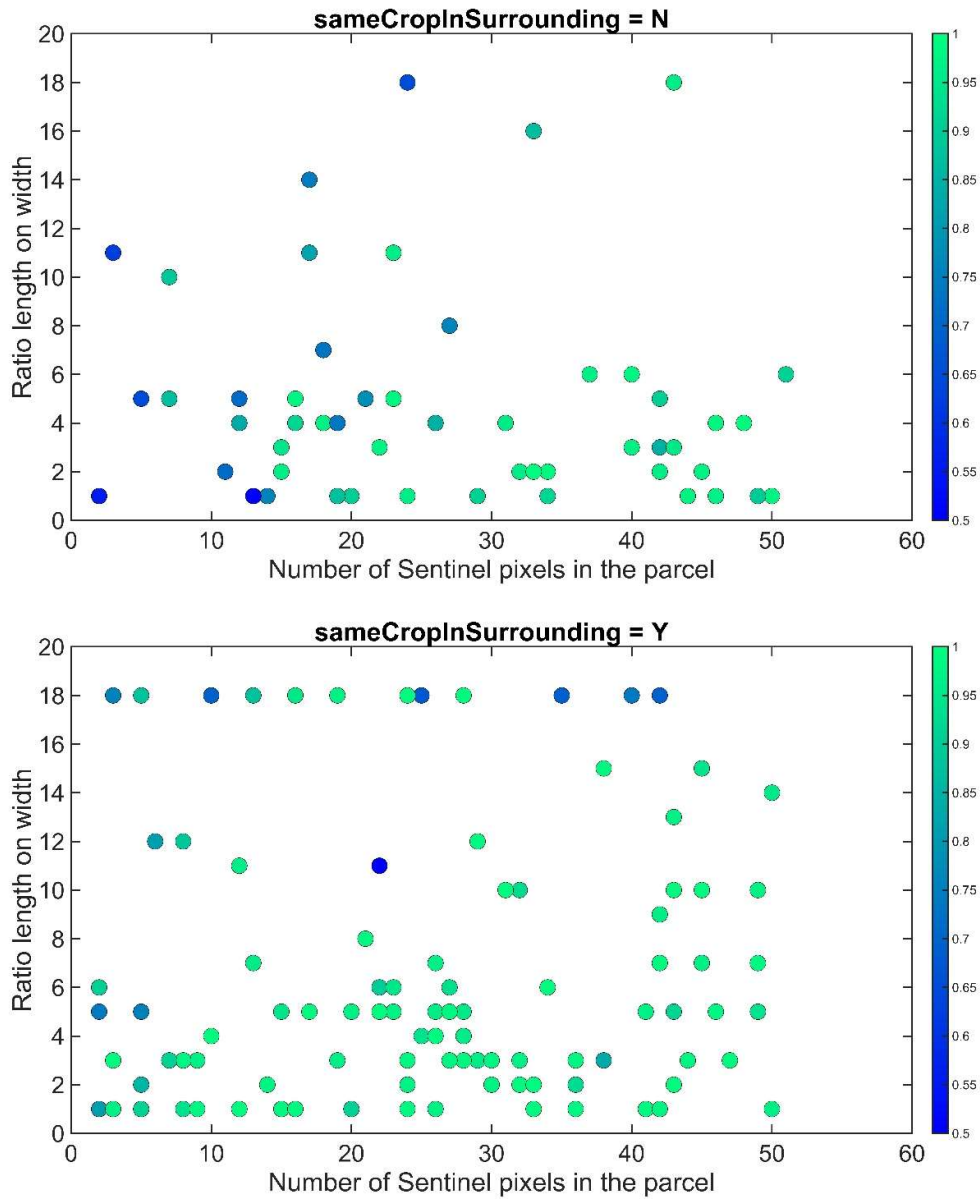


Figure 20. Graph of the correlation coefficient as a function of the number of full S2 pixels and the % of S2 pixels lost after application of 5m negative buffer - the same crop in surrounding. The size of the circles expresses the % lost of pixels after application of the negative buffer on parcels with grass (marked in blue), sugar beet (in yellow), winter wheat (in viola) and maize (in red).

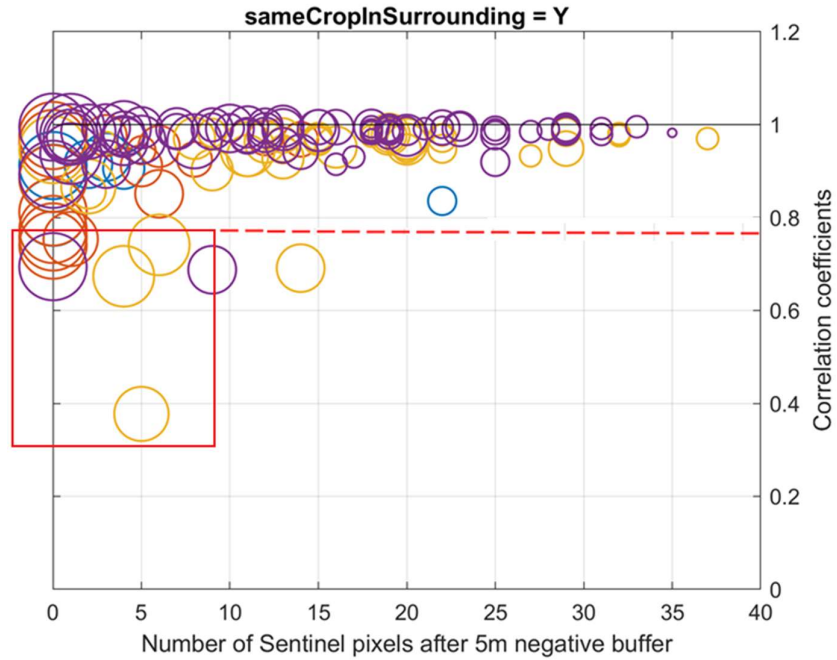


Figure 21. Graph of the correlation coefficient as a function of the number of full S2 pixels and the % of S2 pixels lost after application of 5m negative buffer - for isolated parcel surrounded with different crop. The size of the circles expresses the % lost of pixels after application of the negative buffer on parcels with grass (marked in blue), sugar beet (in yellow), winter wheat (in viola) and maize (in red).

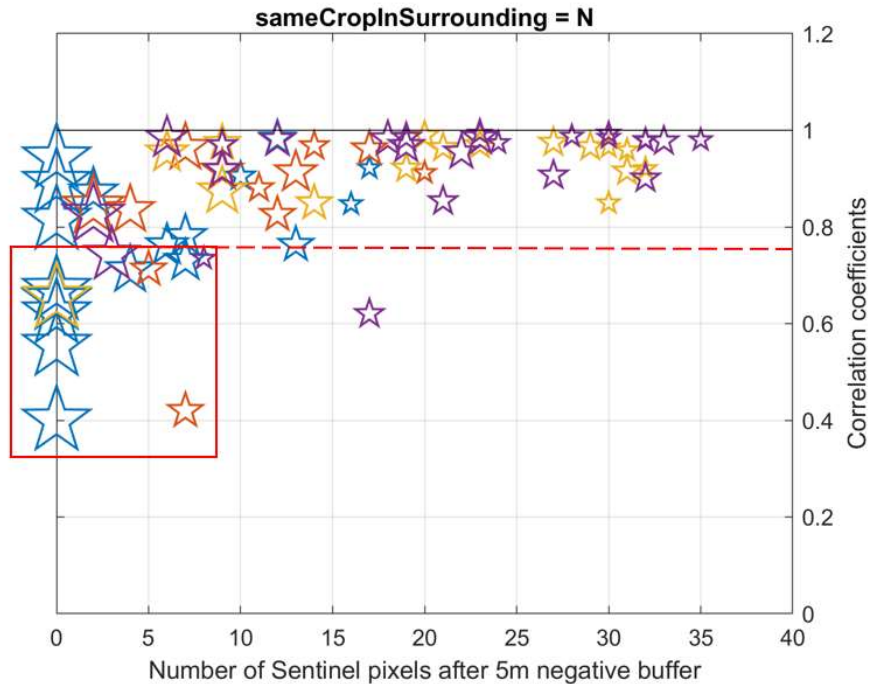


Figure 22. Model quantifying the probability of exceeding the correlation coefficient value of 0.75 as a function of the number of full pixels in the parcel and the percentage of pixels that are lost after application of the 5m buffer – the same crop in surrounding

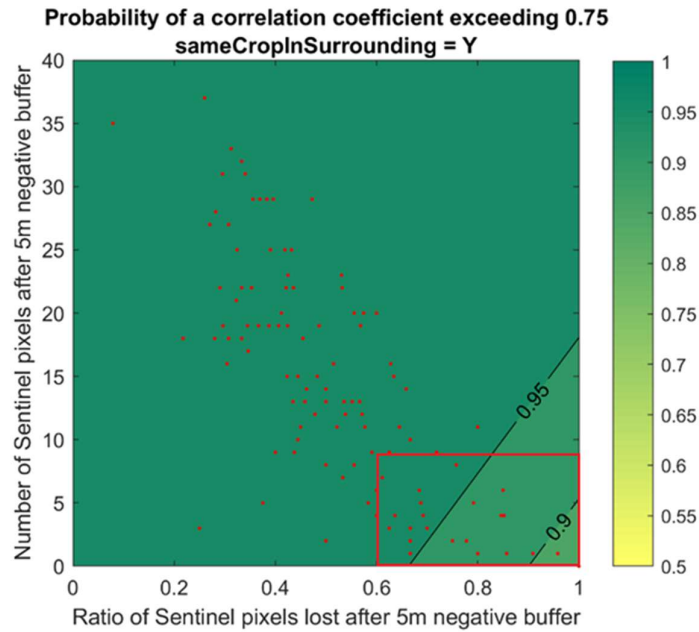
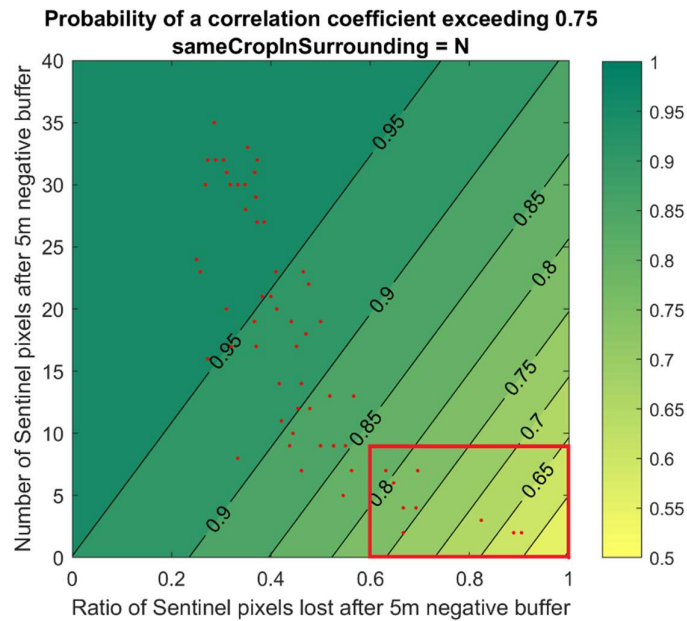


Figure 23. Model quantifying the probability of exceeding the correlation coefficient value of 0.75 as a function of the number of full pixels in the parcel and the percentage of pixels that are lost after application of the 5m buffer – isolated parcels surrounded by different crops.



The probability that the correlation coefficient will exceed the value of 0.75 resulted higher than 80% for all parcels having the same crop as adjacent parcels. For the majority of those parcels, the probability was even higher than 95% (see **Figure 22**). This finding led to the conclusion that the information content of the signal received from the small parcels and amplified with the signal of the adjacent parcels of the same crop (or similar phenology) keeps the NDVI time series similar to the HHR ones. The worst performance was observed for very elongated parcels. These parcels are more vulnerable to the co-registration error of the sensor. If the co-registration shift is in the same or similar direction as the direction of parcel elongation, the Sentinel-2 gives worse performance even if the parcel is surrounded with the same crop. HHR data could bring a benefit in these cases.

A challenge remained for the small parcels with different crop phenology in the surrounding. By analysing these cases, the other two main parameters affecting the similarities were detected. The number of full pixels in the parcels (i.e. the pixels within a 5m negative buffer) and the percentage of pixels that are lost after application of the 5m buffer. Example in **Figure 23** illustrates the dependency of Sentinel-2 performance on both parameters.

The evidences from this study point towards the following assertion: there is a higher possibility that the Sentinel-2 NDVI time series could deviate from the Planet Scope NDVI time series above the acceptable threshold for the parcels where both of the following criteria are met:

- the parcels contain less than 8 full pixels
- the percentage of S2 pixels lost after application of 5m negative buffer is higher than 60%

This threshold is illustrated in figure **Figure 20**, **Figure 21**, **Figure 22** and **Figure 23** by **red box**.

In the tested sample, the set of criteria above represents 25% of the parcels with an average area of 0.12 ha, while the remaining 75% of parcels have an average area of 0.31 ha (see **Table 11**).

Table 10. Analysis of size of the parcels considering the criteria derived from the modelling and expert judgement assessment

Assessment based on the expert judgement																		
Crop	Total number of parcels	Number of deviated parcels	SMALL PARCELS (< 8 clean pixels and > 60% of pixels lost)									OTHERWISE						
			No agreement S2 vs Planet						Agreement S2 vs Planet			No agreement S2 vs Planet			Agreement S2 vs Planet			
			Number of parcels	Area [ha]			Number of parcels	Area [ha]			Number of parcels	Area [ha]			Number of parcels	Area [ha]		
				Min	Mean	Max		Min	Mean	Max		Min	Mean	Max		Min	Mean	Max
Grassland	25	3	3	0.02	0.03	0.03	13	0.02	0.08	0.13	0	NA	NA	NA	9	0.14	0.23	0.37
Maize	29	2	2	0.04	0.05	0.06	10	0.02	0.13	0.26	0	NA	NA	NA	17	0.09	0.21	0.31
Sugar beet	55	4	3	0.22	0.24	0.28	3	0.04	0.18	0.41	1	0.41	0.41	0.41	48	0.05	0.34	0.50
Winter wheat	96	10	2	0.17	0.18	0.18	15	0.03	0.12	0.27	8	0.15	0.33	0.43	71	0.10	0.33	0.50
Arable crops	180	16	7	0.04	0.17	0.28	28	0.02	0.13	0.41	9	0.15	0.34	0.43	136	0.05	0.32	0.50
Total	205	19	10	0.02	0.13	0.28	41	0.02	0.11	0.41	9	0.15	0.34	0.43	145	0.05	0.31	0.50

Table 11. Analysis of size of the parcels considering the criteria derived from the modelling and statistical assessment

Assessment based on the test of the correlation coefficient (>0.5 with 95% confidence level)																		
Crop	Total number of parcels	Number of deviated parcels	SMALL PARCELS (< 8 clean pixels and > 60% of pixels lost)									OTHERWISE						
			No agreement S2 vs Planet						Agreement S2 vs Planet			No agreement S2 vs Planet			Agreement S2 vs Planet			
			Number of parcels	Area [ha]			Number of parcels	Area [ha]			Number of parcels	Area [ha]			Number of parcels	Area [ha]		
				Min	Mean	Max		Min	Mean	Max		Min	Mean	Max		Min	Mean	Max
Grassland	25	9	6	0.02	0.05	0.13	10	0.02	0.07	0.13	3	0.14	0.2	0.28	6	0.18	0.24	0.37
Maize	29	5	3	0.02	0.04	0.06	9	0.02	0.14	0.26	2	0.12	0.13	0.14	15	0.09	0.22	0.31
Sugar beet	55	5	4	0.22	0.35	0.41	2	0.04	0.07	0.09	1	0.41	0.41	0.41	48	0.05	0.34	0.50
Winter wheat	96	5	2	0.08	0.13	0.18	15	0.03	0.12	0.27	3	0.15	0.26	0.33	76	0.1	0.33	0.50
Arable crops	180	15	9	0.02	0.20	0.41	26	0.02	0.12	0.27	6	0.12	0.24	0.41	139	0.05	0.32	0.50
Total	205	24	15	0.02	0.14	0.41	36	0.02	0.11	0.27	9	0.12	0.28	0.41	145	0.05	0.32	0.50

It is important to note that in the case of grassland, it is expected that the time series derived from different data may differ more due to the actual land management; mown areas may have a marked pattern but grazed areas should not show any disruption over time. In the selected sample, the grassland parcels were all permanent grazed areas, therefore, using correlation coefficient to assess the similarity is not appropriate. Research for an alternative method will be performed in 2019. For the moment, the results on grassland are not included in the following extra analysis, as they, although similar, could give misleading conclusions. Therefore, in **Table 10** and **Table 11** the results are presented separately for arable crops (highlighted in orange) and for the overall result (highlighted in red) including also the permanent grasslands.

For the 180 parcels representing the arable crops, the summary statistics for the automatic analysis of the correlation coefficient are presented in **Table 12**.

Table 12. Summary statistics – percentage of deviations of the S2 NDVI comparing to the NDVI derived from Planet, observed for different groups of parcels

	“Small parcels” (according to the criteria)	Other parcels
Composition in the remaining sample	35	145
Parcels for which the S2 NDVI data deviate from the NDVI derived from Planet [%]	26%	4%
Total of parcels for which the S2 NDVI data deviate from the NDVI derived from Planet [%]	9% from the whole sample of 180 parcels (considered arable crop only)	

The proportions of deviations for each group in **Table 12** confirm the correctness of above set limit criteria. The group of “small parcels” (i.e. parcels with less than 8 pixels and more than 60% loss) is much more sensitive to our similarity assessment (26% deviate) than the rest (i.e. more than 8 pixels and less than 60% loss) where the deviation was observed just for 4% of parcels.

Unfortunately, the set of small parcels (according to the criteria) was too limited to develop a similar model for estimation of limits of the HHR imagery. Since the criteria determined for Sentinel-2 are independent on the GSD of the sensor, the hypothesis of using the same rules could be applied for the satellites with similar geometric positional accuracy. However, in the selected sample only 1 parcel meets the criteria at the Planet scale (i.e. less than 8 full Planet pixels and more than 60% of pixel loss after application of 1.5m negative buffer, i.e 0.5*pixel size). Therefore, an analysis on the bigger sample of data would be needed to confirm or decline the assumption.

6 Discussion & Conclusions

6.1 Summary of specific findings related to the sample:

1. The Sentinel-2 NDVI signal deviates from the NDVI signal retrieved from Planet Scope imagery for not more than 12%, out of 205 small agriculture parcels.
2. The Sentinel-2 NDVI signal deviates from the NDVI signal retrieved from Planet Scope imagery for not more than 9%, out of 180 small agriculture parcels with arable crop only (without permanent grassland).
3. Based on visual assessment, all HHR NDVI time series that deviate from S2 ones bring an added value to the interpretation of markers.
4. There is a strong probability that the Sentinel-2 NDVI time series could deviate from the Planet Scope NDVI time series above the acceptable threshold for parcels that:
 - contain less than 8 full pixels and at the same time
 - the percentage of S2 pixels lost after application of 5m negative buffer is higher than 60%.
5. Unfortunately applying the same model at the Planet scale to understand the limits of this HHR sensor did not bring any results due to the lack of such small parcels in the sample.

6.2 General conclusions and discussion

The evidence from this study suggests that the size of the parcel expressed as an area in metric units is not an appropriate measure to define the 'small parcel' in the context of CAP checks by monitoring. Another two geospatial parcel parameters instead seem to manifest the correlation with the ability of the sensor to provide interpretable NDVI signal providing expected information. These parameters are: 1) number of full pixels remaining after application of a buffer, expressing both the size of the parcel and the position of the parcel regards to the raster; 2) the percentage of pixels lost after application of the same buffer, considering the shape and position of the parcels regards to the raster.

The low accuracy of Sentinel-2 cloud cover mask provided as a part of the product influenced the size of the tested sample. Fully automated processing based on the cloud cover metadata attached to the product would bring unwanted noise into the analysed NDVI signal, which would have a negative impact on both the overall performance of Sentinel-2 signal and the accuracy of the final criteria resulting from the modelling phase. In order to ground our analysis on plausible NDVI time series we decided to perform assure high quality results by semi-automatic fine-tuning consisting in cleaning of the NDVI signal from pixels still effected by clouds and shadows. Although the study was performed on a limited sample of parcels, it demonstrated that the Sentinel-2 imagery can capture sufficient signal in most of the cases, and the need for HHR imagery as an alternative source of data should be limited.

The limitation of the applied methodology consist in fact that the correlation coefficient used to assess the deviation between the pair of NDVI time series is a measure of the direction and strength of the linear relationship between two variables. Hence, its application is not suitable for crops for which phenology (or activity on the field) is represented by a flat NDVI profile (without characteristic points). In this study, the permanent grassland grazed by animals is one of such cases.

In order to understand whether the same limiting criteria could be used also for the HHR sensor, we suggest to gather the representative sample of very small parcels (i.e less than 8 pixel size in PlanetScope scale) and to perform the same methodology.

Since the accurate cloud cover mask is fundamental for the automated cloud processing of big data and subsequent correct interpretation and evaluation of results, an intensive effort is required to improve the recognition of unwanted pixels on a reliable level. Once the metadata related to this issue provides reliable information, the tested sample could be

easily extended to thousands of parcels. In that case using the same methodology to determine the criteria of small parcels, either for Sentinel-2 or other HHR sensor, could be further refined on. Additionally, the influence of other parameters like landscape characteristics could be analysed.

References

1. Technical guidance on the decision to go for substitution of OTSC by monitoring; DS/CDP/2018/17
2. https://earth.esa.int/documents/247904/685211/Sentinel-2_User_Handbook
3. <https://earth.esa.int/web/sentinel/user-guides/sentinel-2-msi/product-types/level-2a>
4. <https://earth.esa.int/web/sentinel/user-guides/sentinel-2-msi/product-types/level-1c>
5. <https://www.planet.com/products/satellite-imagery/planetscope-analytic-ortho-scene/>
6. <https://qgis.org/api/classQgsRasterCalculator.html>
7. <https://qgis.org/api/classQgsZonalStatistics.html>
8. <https://www.qgis.org/en/site/>
9. Atmospheric corrections – Fundamentals, ESA advanced training course on land remote sensing, http://seom.esa.int/landtraining2015/files/Day_2/D2T1b_LTC2015_Gastellu-Etchegorry.pdf
10. Rosa Coluzzi, Vito Imbrenda, Maria Lanfredi, Tiziana Simoniello, A first assessment of the Sentinel-2 Level 1-C cloud mask product to support informed surface analyses, Remote sensing of environment, Volume 217, November 2018, Pages 426-443, <https://doi.org/10.1016/j.rse.2018.08.009>
11. S. Clerc, O. Devignot, L. Pessiot, S2 MPC TEAM, S2 MPC L1C Data Quality Report – 08/10/2018, (2018)
12. SOILLE Pierre, BURGER Armin, DE MARCHI Davide, HASENOHR Paul, KEMPENEERS Pieter, RODRIGUEZ ASERETTO Roque Dario, SYRRIS Vasileios, VASILEV Veselin, The JRC Earth Observation Data and Processing Platform, Big data from Space, <https://ec.europa.eu/jrc/en/publication/proceedings-2017-conference-big-data-space>
13. https://marswiki.jrc.ec.europa.eu/wikicap/index.php/Positional_Accuracy
14. https://www.planet.com/products/satelliteimagery/files/Planet_Combined_Imagery_Product_Specs_December2017.pdf
15. Lemajic, S, Vajsova, B., Aastrand, P., New sensors benchmark report on PlanetScope, PUBSY JRC 111221, EUR 29319 EN, ISBN 978-92-79-92833-8, ISSN 1831-9424, doi: 10.2760/178918, 2018. Available online: <http://publications.jrc.ec.europa.eu/repository/handle/JRC111221>
16. ASPRS Positional Accuracy Standards for Digital Data, ©2014 American Society for Photogrammetry and Remote Sensing, doi: 10.14358/PERS.81.3.A1-A26
17. R.A. Fisher (1944). Statistical methods for research workers (9th edition). Edinburgh, London: Oliver and Boyd Ltd.
18. <http://www.nationaalgeoregister.nl>

List of abbreviations

AOI	Area Of Interest
BOA	Bottom Of Atmosphere
CAP	Common Agricultural Policy
CC	Cloud Cover
CE(xx)	Circular Error at xx % confidence level
ESA	European Space Agency
EU	European Union
GSAA	Geospatial Aid Application
HHR	High High Resolution
JEODPP	JRC Earth Observation Data and Processing Platform
GCPs	Ground Control Points
GSD	Ground Sampling Distance
GRI	Global Reference Image
L2A	Level-2A
L1C	Level-1C
LPIS	Land Parcel Identification System
MS(s)	Member State(s)
NDVI	Normalized Difference Vegetation Index
NIR	Near Infra-Red
OTSC	On The Spot Checks
RMSE	Root Mean Square Error
S2	Sentinel-2
S2A	Sentinel-2A
S2B	Sentinel-2B
SCL	Scene Classification Layer
SR	Surface Reflectance
TOA	Top Of Atmosphere

List of figures

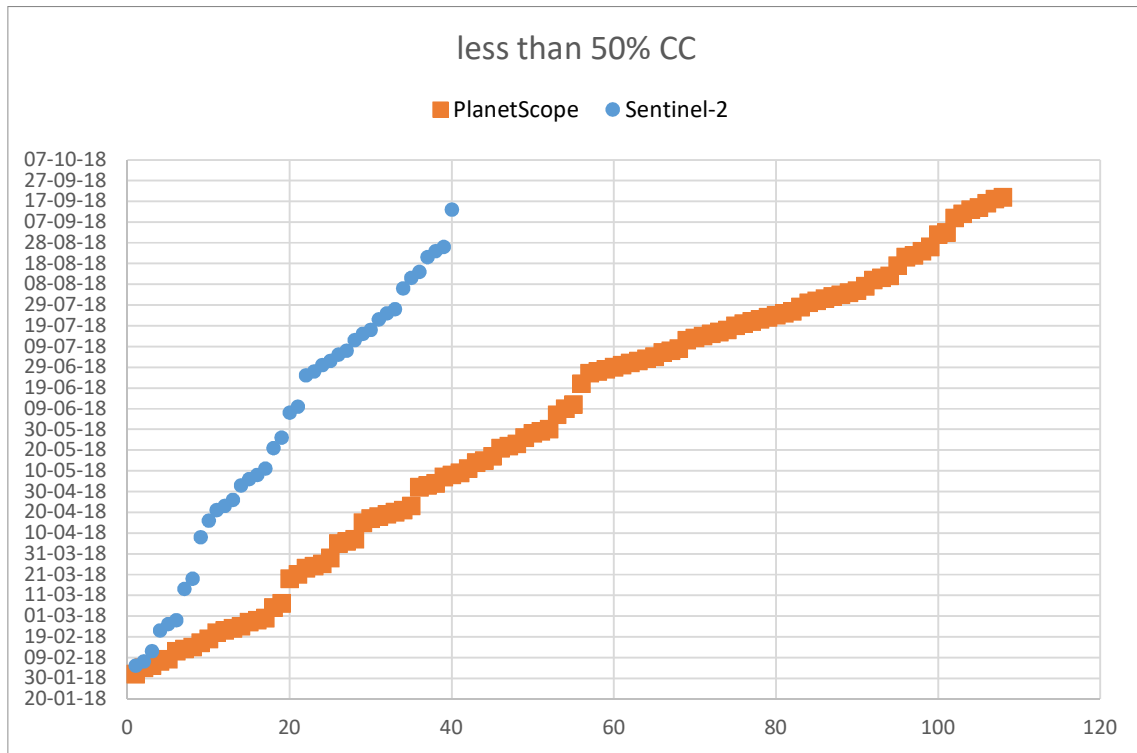
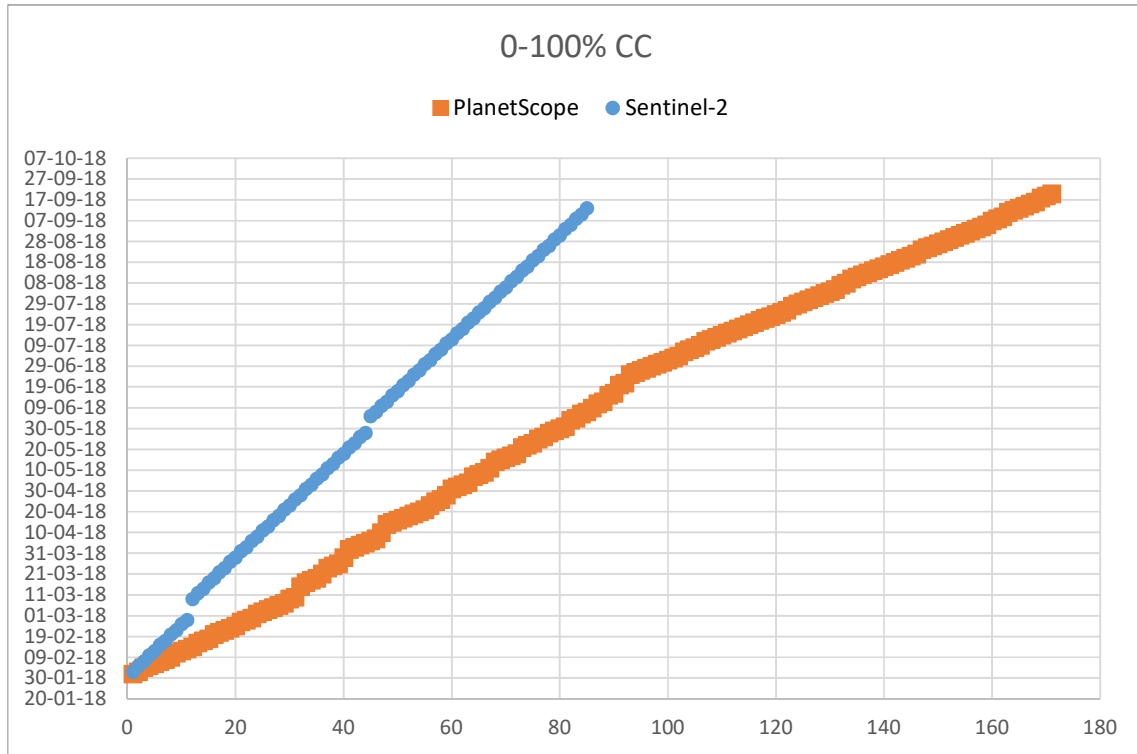
Figure 1. Concept of case study	1
Figure 2. Position of the AOIs in Netherlands	3
Figure 3. Different shape types representing the sample	4
Figure 4. Position of the parcel on the raster and different number of pixels inside the parcel	6
Figure 5. Example of the negative buffer and the subsequent number of full pixels.....	7
Figure 6. Influence of negative buffer on the mean NDVI time series – Maize	7
Figure 7. Influence of the negative buffer on the mean NDVI time series - Grassland ...	8
Figure 8. False colour composite (RGB 421) of a Planetscope image acquired on 15/05/2018 over AOI-1 mosaicked from 7 ortho scene tiles.....	9
Figure 9. NDVI image calculated from Planetscope data acquired on 15/05/2018 over AOI1	10
Figure 10. Example of the geometric positional inaccuracy of raster data	11
Figure 11. Validation graph –maize	17
Figure 12. Validation graph -grassland.....	17
Figure 13. Validation graph – winter wheat	18
Figure 14. Validation graph –sugar beet.....	18
Figure 15. Example of NDVI time series – added/no added value of HHR (Maize).....	19
Figure 16. Example of NDVI time series – added/no added value of HHR (Grassland) ..	19
Figure 17. Example of NDVI time series – added/no added value of HHR (Winter wheat)	20
Figure 18. Example of NDVI time series – added/no added value of HHR (Sugar beet)	20
Figure 19. Graph of the correlation coefficient (colour scale) as a function of the shape of the parcels and the % of S2 pixels lost after application of 5m negative buffer. Top: isolated parcels surrounded by different crops; bottom: parcels with the same crop around.....	22
Figure 20. Graph of the correlation coefficient as a function of the number of full S2 pixels and the % of S2 pixels lost after application of 5m negative buffer - the same crop in surrounding. The size of the circles expresses the % lost of pixels after application of the negative buffer on parcels with grass(marked in blue), sugar beet (in yellow), winter wheat (in viola) and-maize (in red).	23
Figure 21. Graph of the correlation coefficient as a function of the number of full S2 pixels and the % of S2 pixels lost after application of 5m negative buffer - for isolated parcel surrounded with different crop. The size of the circles expresses the % lost of pixels after application of the negative buffer on parcels with grass(marked in blue), sugar beet (in yellow), winter wheat (in viola) and-maize (in red).....	23
Figure 22. Model quantifying the probability of exceeding the correlation coefficient value of 0.75 as a function of the number of full pixels in the parcel and the percentage of pixels that are lost after application of the 5m buffer – the same crop in surrounding	24
Figure 23. Model quantifying the probability of exceeding the correlation coefficient value of 0.75 as a function of the number of full pixels in the parcel and the percentage of pixels that are lost after application of the 5m buffer – isolated parcels surrounded by different crops.	24

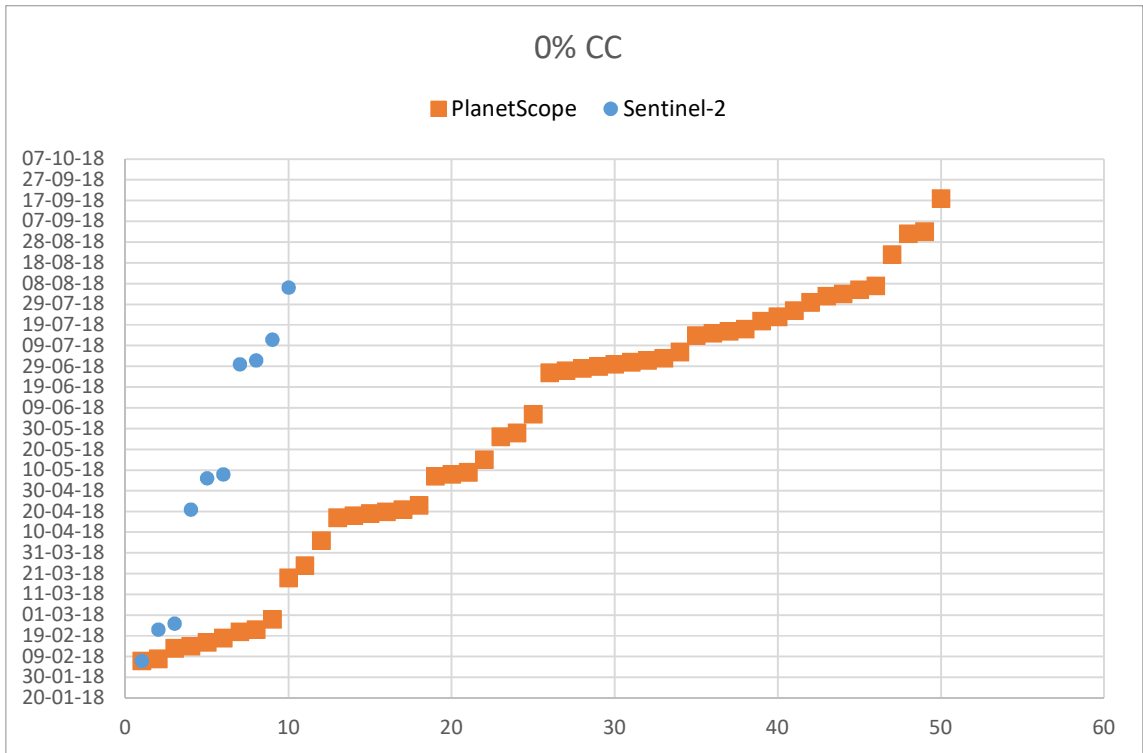
List of tables

Table 1. Setting critical thresholds on parcels size for Sentinel-2 data	1
Table 2. Setting critical thresholds on parcels size for HHR data	1
Table 3. Availability of the products according to the search criteria.....	3
Table 4. Distribution of shape types according to the parcel size	4
Table 5. Distribution of tested crops.....	5
Table 6. Distribution of tested crops according to the processing level of Sentinel-2 data	5
Table 7. Estimated parameters of the regression model and their significant tests	16
Table 8. The summary assessment table based on the visual assessment - number of parcels where the signal of Sentinel-2 deviates from the Planet's signal	21
Table 9. The summary assessment table based on the statistical assessment - % of parcels where the signal of Sentinel-2 deviates from the Planet's signal	21
Table 10. Analysis of size of the parcels considering the criteria derived from the modelling and expert judgement assessment	26
Table 11. Analysis of size of the parcels considering the criteria derived from the modelling and statistical assessment	26
Table 12. Summary statistics – percentage of deviations of the S2 NDVI comparing to the NDVI derived from Planet, observed for different groups of parcels.....	27

ANNEX A

Comparison between PlanetScope and Sentinel-2 data availability





GETTING IN TOUCH WITH THE EU

In person

All over the European Union there are hundreds of Europe Direct information centres. You can find the address of the centre nearest you at: https://europa.eu/european-union/contact_en

On the phone or by email

Europe Direct is a service that answers your questions about the European Union. You can contact this service:

- by freephone: 00 800 6 7 8 9 10 11 (certain operators may charge for these calls),
- at the following standard number: +32 22999696, or
- by electronic mail via: https://europa.eu/european-union/contact_en

FINDING INFORMATION ABOUT THE EU

Online

Information about the European Union in all the official languages of the EU is available on the Europa website at: https://europa.eu/european-union/index_en

EU publications

You can download or order free and priced EU publications from EU Bookshop at: <https://publications.europa.eu/en/publications>. Multiple copies of free publications may be obtained by contacting Europe Direct or your local information centre (see https://europa.eu/european-union/contact_en).

The European Commission's science and knowledge service

Joint Research Centre

JRC Mission

As the science and knowledge service of the European Commission, the Joint Research Centre's mission is to support EU policies with independent evidence throughout the whole policy cycle.



EU Science Hub

ec.europa.eu/jrc



@EU_ScienceHub



EU Science Hub - Joint Research Centre



Joint Research Centre



EU Science Hub



Publications Office

doi:10.2760/26277

ISBN 978-92-76-01935-0